University of California
Los Angeles

Self-Similar Blowup Solutions of the Aggregation Equation

A dissertation submitted in partial satisfaction
of the requirements for the degree
Doctor of Philosophy in Mathematics

by

Yanghong Huang

2010

© Copyright by
Yanghong Huang
2010

The dissertation of Yanghong Huang is approved.

Warren B. Mori

Russel Caflisch

Chris Anderson

Andrea L. Bertozzi, Committee Chair

University of California, Los Angeles

2010

To my grandma, who guided me on the straight and narrow path for my whole life.

Table of Contents

List of Figures

List of Tables

Acknowledgments

Foremost, I would like to thank my advisor, Professor Andrea Bertozzi, for her continuous guidance and generous support throughout my graduate studies at UCLA, and encouragement to attend conferences and workshops and to interact with other researchers. I learned not only numerous ideas and ways to conduct research, but also many other thing beyond academics.

I would also like to thank many other professors I learned a lot from: various topics in the seminars organized by Professor Chris Anderson; kinetic theory and multiscale methods from Professor Russel Caflisch; numerous techniques in linear and nonlinear PDEs, theory of viscosity solutions and optimal transport, and free and moving boundary problems from Professor Inwon Kim; the level set method and related schemes for conservation laws and Hamilton-Jacobi equations from Professor Stanley Osher; techniques in perturbation and asymptotics, theory of magnetohydrodynamics and turbulence from Paul Roberts.

I would like to express my gratitude to my committee member Professor Warren Mori and I benefited from a lot of activities organized by Institute for Digital Research Education (IDRE) directed by him. I am also grateful to Professor Eli Yablonovitch for many daily life examples where theoretical knowledge is applied. I would like to thank Professor Tom Witelski for collaboration on the shooting method and many valuable discussions.

I would like to thank the staff, especially Maggie, Martha and Babette, for their help to make the graduate life as comfortable as possible.

I am fortunate to get to know so many friends at UCLA. My special thank goes to Jinjun Xu, who is like a brother for the past few year.

Finally, I would like to thank my parents, my younger sister and brother in China, whom this thesis is dedicated to.

This work is supported by NSF DMS-0907931, Dynamics of aggregation and collapse in multidimensional swarming models.

Vita

1981	Born, Shuangfeng, Hunan Province, China
2004	B.S. (Mathematics), Hong Kong Baptist University.
2006	M.A. (Mathematics), University of California, Los Angeles

Publications

Yanghong Huang and Andrea Bertozzi. Self-similar blowup solutions to an aggregation equation in R^N. SIAM J. Appl. Math., 70(7):2582-2603(2010)

Andris M. Dimits , Chiaming Wang , Russel Caflisch , Bruce I. Cohen and Yanghong Huang. Understanding the accuracy of Nanbu's numerical Coulomb collision operator. Journal of Computational Physics, 228(13): 4881-4892, 2009

Zhijun Tan and Yanghong Huang, An alternating Crank-Nicolson method for the numerical solution of the phase-field equations using adaptive moving meshes, International Journal for Numerical Methods in Fluids, 56(9): 1673-1693, 2008.

Yanghong Huang, Optimal Design for the Grating Coupler of Surface Plamons. Proceedings of the COMSOL Users Conference 2008, 4 pages, Boston.

Abstract of the Dissertation

Self-Similar Blowup Solutions of the Aggregation Equation

by

Yanghong Huang

Doctor of Philosophy in Mathematics

University of California, Los Angeles, 2010

Professor Andrea L. Bertozzi, Chair

In this work, we consider various self-similar solutions of the aggregation equation $u_t = \nabla \cdot (u \nabla K * u)$ with the special homogeneous kernel $K(x) = |x|^\gamma$. Depending on the power γ, different self-similar solutions are investigated.

When $\gamma = 2$, there is an explicit formula for the solution, which is an simple rescaled function of the initial solution.

When $\gamma \in (0, 2)$, any smooth solution blows up in finite time. Motivated by some previous work on the non-existence of self-similar solutions of the first kind, we show that the self-similar solutions are of the second kind, using high resolution numerics and different ways to reduce the computational effort as small as possible. The blowup profiles and their *anomalous* exponents are calculated by post-processing of the numerical data of the blowup dynamics. Even though there is no explicit formula for it, the anomalous exponent can be retrieved in odd dimensions for the special kernel $K(x) = |x|$. In this case, the original PDE is transformed into a system of ODEs, and a shooting method is used to find the optimal parameters to match the desired far field condition. In addition, the limiting behavior when the power γ goes to zero is studied, giving more insights

of these self-similar solutions for the general cases.

When $\gamma \in (2, \infty)$, any smoothing solution remains smooth and only blows up at infinite time. The main technique used is a similarity transform originating from dimensional analysis, resulting in another equation with better properties. This transformed equation is studied in detail, from the qualitative characterization of the limits for general solutions to quantitative asymptotics of the convergence to the singular limits for radially symmetric solutions. For smooth, radially symmetric initial data, the solution of the transformed equation converges to a Dirac δ-ring, whose radius is determined by the total initial mass, the power γ and the dimension of the space. The predicted asymptotic behavior of convergence is in excellent agreement with the numerical simulation of the PDEs.

CHAPTER 1

Introduction and Background

1.1 Physical Background of the Aggregation-Type Equations

The aggregation equation

$$u_t = \nabla \cdot (u \nabla K * u) \tag{1.1}$$

arises in a number of context in biological models and physical applications. Here u is usually the mass density of the species or material and $K*u$ is the convolution of u with some kernel K. In biology, the swarming mechanism can be described by this equation in which individuals sense the presence of others. A related equation with the kernel $K(x) = e^{-|x|}$ is used to simulate the aggregation of nano-particles by Holm and Putkaradze [HP05, HP06]. At the individual level, this aggregation mechanism can be described by a system of ODEs [BCM00, CHD07, MCO05, OL01] and only the simplest case relevant to the continuum models is reviewed here. Let $\{x_1, x_2, \cdots, x_L\}$ be the position of the L particles representing the individuals with mass $\{m_1, m_2, \cdots, m_L\}$. Assuming that the pairwise interaction between two particles x_i and x_j, or more precisely the relative velocity between them, is proportional to

$$-\nabla K(x_i - x_j), \tag{1.2}$$

then the velocity of a specific particle is simply

$$\frac{d}{dt}x_i = -\sum_{j\neq i} m_j \nabla K(x_j - x_i). \tag{1.3}$$

In general the only assumption on the kernel K is the symmetry $K(-x) = K(x)$ under reflection. Very often the underlying environment or medium is assumed to be homogeneous and rotationally invariant, reflected in the symmetry of the kernel $K(x) = k(|x|)$ for for some function k. Therefore above equation can be rewritten as

$$\frac{d}{dt}x_i = -\sum_{j\neq i} m_j \frac{x_j - x_i}{|x_j - x_i|} k'(|x_j - x_i|). \tag{1.4}$$

When the number of particles L becomes large, the particles can be modeled as a continuum, with a mass density u, giving the continuous equation (1.1) above. The properties of both of the discrete and continuum equation are reviewed in the next chapter.

Related equation also used to model over-damped gravitational interaction of a cloud of particles and chemotaxis in bacteria is the Keller-Segel equation [KS70]

$$\partial_t \rho = \Delta\rho - \nabla \cdot (\rho \nabla c), \tag{1.5a}$$

$$-\Delta c = \rho, \tag{1.5b}$$

where ρ is the density of the cloud or the bacteria and c represents the gravitational potential or the density of the chemo-attractant. In spatial dimension greater than two, there are at least two types of blowup solutions (see [BCK99]). One is exactly self-similar, concentrating zero mass in the core of the blowup profile, and the other is like a Burgers shock, with finite mass in a ring converging to the origin.

Another closely related equations appear in the modeling of the self-aggregation of finite-size particles [HP05, HP06], different from the standard Debye-Hückle [DH] or Keller-Segel [KS70] model. Let the local density of the particles be ρ, then the evolution equation can be written as

$$\frac{\partial \rho}{\partial t} = -\nabla \cdot \mathbf{J}, \quad \text{with } \mathbf{J} = -D\nabla\bar{\rho} - \mu(\bar{\rho})\rho\nabla\Phi, \tag{1.6}$$

where D is the diffusion coefficient, $\bar{\rho}$ is the averaged density of ρ, μ is the density-dependent mobility and Φ is the potential. The non-local interaction between these particles are characterized by Φ by

$$\Phi(\mathbf{r}) = -\int \rho(\mathbf{r}')G(|\mathbf{r} - \mathbf{r}'|)d\mathbf{r} \tag{1.7}$$

for some kernel G. Numerical simulations of (1.6) shows the coexistence of the steady state solutions as well as the collapse of solutions from smooth initial data in two and three dimensions.

In the absence of diffusion, all the equations considered above fall into the much more general *active scalar problem* [Con94] for the transport of a scalar quantity. The corresponding equation can be written as

$$\frac{\partial \rho}{\partial t} - \nabla \cdot (\rho\vec{v}) = 0, \quad \vec{v} = \vec{K}_1 * \rho + \nabla K_2 * \rho, \tag{1.8}$$

where ρ is the scalar to be convected and $\vec{K}_1$ is a divergence-free (or incompressible) vector kernel. This type of problem roots in classical theory of fluid dynamics, including two dimensional vortex dynamics [MB02, Yud63] and quasi-geostrophic equation [CMT94], in which the transport velocity is divergence free. In the vorticity-stream formulation of the Euler equation in two dimension, ρ is the vorticity and the kernel $\vec{K}_1(x)$ is $\dfrac{(x_2, -x_1)}{2\pi|x|^2}$ while in the quasi-geostrophic model, the kernel $\vec{K}_1$ is the fractional Laplacian $\nabla^{\perp}(-\Delta)^{-\alpha}$. On the other hand, most models for the aggregation of a swarm have a velocity that is a gradient. The model with both divergence-free part and gradient part is studied in two dimensional vortex motion in superconductors [DZ03], and in a two-dimensional kinematic model for swarming pattern [TB04]. The latter is inspired by a one-dimensional model with both odd and even nonlocal interactive kernels [ME99].

1.2 General Theory for Self-similar Solutions

The main contributions of this thesis are the understanding of self-similar dynamics of blowup in multi-dimensional aggregation equations. These self-similar solutions, if they exist, are intimately related to the invariance of equations under scaling transformation. Therefore in the following we review some fundamental ideas for self-similarity in PDEs.

1.2.1 Dimensional Analysis, Scaling and Similarity Transform

The fundamental idea of dimensional analysis is that physical laws do not depend on any chosen basic units of measurements. More specific, let a_1 be any physical quantity that depends on the basic quantities L_1, M_1 and T_1 in one basic units of measurements, i.e.

$$a_1 = \phi(L_1, M_1, T_1). \tag{1.9a}$$

Similarly, the corresponding quantity in another basic units of measurements is

$$a_2 = \phi(L_2, M_2, T_2). \tag{1.9b}$$

The principle of dimension analysis means that

$$\frac{a_1}{a_2} = \frac{\phi(L_1, M_1, T_1)}{\phi(L_2, M_2, T_2)} = \phi\left(\frac{L_1}{L_2}, \frac{M_1}{M_2}, \frac{T_1}{T_2}\right). \tag{1.10}$$

As a result, the function ϕ must be a power-law monomial, i.e.

$$\phi(L, M, T) = CL^\alpha M^\beta T^\gamma, \tag{1.11}$$

for some constants C, α, β and γ. One example is the Newton's second law in either the MKS or CGS system.

The principle of dimensional analysis has been used for a long time, starting from Newton and Fourier to Maxwell, Rayleigh, Reynolds and Kolmorogov. Any derived equation for physical phenomena should have consistent dimensions for all individual terms. More importantly, dimensional analysis can greatly simplify the presentation of solutions to equation, summarized by the celebrated Buckingham $\prod$ theorem [Bar96]:

Theorem 1.2.1. *Let a be a function of $n+m$ variables, a_1, $\cdots$,a_n, b_1, $\cdots$, b_m, i.e.*

$$a = f(a_1, a_2, \cdots, b_m). \tag{1.12}$$

If a_1, a_2, $\cdots$, a_n have independent dimensions and a, b_1, b_2, $\cdots$, b_m are expressible in terms of the dimensions of a_1, a_2, $\cdots$, a_n as

$$\begin{aligned}
[a] &= [a_1]^p \cdots [a_n]^r, \\
[b_1] &= [a_1]^{p_1} \cdots [a_n]^{r_1}, \\
&\vdots \\
[b_m] &= [a_1]^{p_m} \cdots [a_n]^{r_m}.
\end{aligned} \tag{1.13}$$

Define the dimensionless numbers

$$\prod = \frac{a}{a_1^p \cdots a_n^r}, \tag{1.14a}$$

$$\prod\nolimits_1 = \frac{b_1}{a_1^{p_1} \cdots a_n^{r_1}}, \tag{1.14b}$$

$$\vdots$$

$$\prod\nolimits_m = \frac{b_m}{a_1^{p_m} \cdots a_n^{r_m}}. \tag{1.14c}$$

Then there exists an function Φ of only m variables, such that

$$\prod = \Phi(\prod_1, \cdots, \prod_m). \tag{1.15}$$

In other words, f can be written as the following simplified form

$$f(a_1, a_2, \cdots, b_m) = a_1^p \cdots a_n^r \Phi\left(\frac{b_1}{a_1^{p_1} \cdots a_n^{r_1}}, \cdots, \frac{b_m}{a_1^{p_m} \cdots a_n^{r_m}}\right). \tag{1.16}$$

The transformation (1.14) from the original variables to the dimensionless variables is call a *similarity transform*. In many situations, we are more interested in the singular behavior of the solution Φ when some of the dimensionless variables go to zero or infinity, corresponding to the large time behavior or finite time blowup limit. Depending on the nature of this limit, we have self-similar solutions of the different kinds, as discussed in the following subsection.

1.2.2 Self-similar Solutions: the First Kind and the Second Kind

Without loss of generality, we consider the limit of the function Φ when $\prod_m$ goes to zero. To illustrate this limiting process, we use the example of measuring the length of a curve in a two-dimensional plane. Depending on the curve, there are three possibilities

- The limit

$$\lim_{\prod_m \to 0} \Phi\left(\prod_1, \cdots, \prod_m\right) = \Phi_1\left(\prod_1, \cdots, \prod_{m-1}\right) \tag{1.17}$$

  exists for some function Φ_1. In this case the solution possesses *complete similarity* and we call the resulting self-similar solution is of the *first kind*. When we approximate the perimeter of the circle of radius R by a regular N-gon with side length $\eta = R \sin \frac{2\pi}{N}$, the perimeter of the polygon is given by

$$L_\eta = N\eta = \frac{2\pi\eta}{\arcsin(\eta/R)} = R\Phi(\prod_1), \tag{1.18}$$

where $\prod_1 = \eta/R$ and $\Phi(\prod_1) = 2\pi \prod_1 / \arcsin(\prod_1)$. The limit of L_η when $\prod_1 = \eta/R$ goes to zero exists and is

$$\lim_{\eta \to 0} L_\eta = R \lim_{\prod_1 \to 0} \Phi(\prod_1) = 2\pi R, \tag{1.19}$$

exactly the perimeter of the circle with $\Phi_1 \equiv 2\pi$.

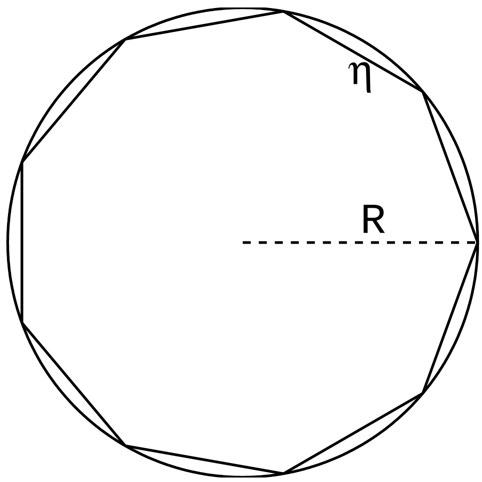

Figure 1.1: The perimeter of a circle approximated by a polygon. The limit when η goes zero exists, which is exactly the perimeter of the circle.

- The above limit does not exist, but instead the limit

$$\lim_{\prod_m \to 0} \frac{1}{\prod_m^\alpha} \Phi\left(\frac{\prod_1}{\prod_m^{\alpha_1}}, \cdots, \frac{\prod_m}{\prod_m^{\alpha m}}\right) = \Phi_1\left(\prod_1, \cdots, \prod_{m-1}\right) \tag{1.20}$$

exists. In this case the solution possesses *incomplete similarity* and we call the resulting self-similar solution is of the *second kind*. When we approximate the perimeter of the fractal—Koch snowflake shown below, using the basic length scale $\eta = R/3^K$ for any integer K, the resulting length is

$$L_\eta = 3R\left(\frac{R}{\eta}\right)^\alpha = R\Phi(\prod_1), \tag{1.21}$$

where $\prod_1 = \eta/R$, $\Phi(\prod_1) = \prod_1^{-\alpha}$ and $\alpha = (\ln 4 - \ln 3)/\ln 3 \approx 0.26$ is the fractal dimension. Obvious the limit of Φ when $\prod_1$ goes to zero does not exits; the actual limit that does exist is

$$\lim_{\prod_1 \to 0} \prod_1^{\alpha} \Phi(\prod_1) = \Phi_1 \equiv 3R. \tag{1.22}$$

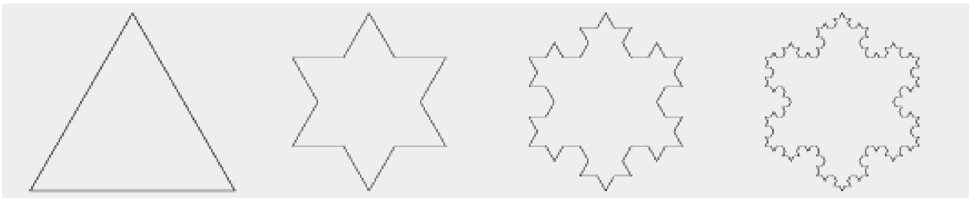

Figure 1.2: Kock snowflake. The perimeter depends on the scale we measure it, but the dependence has a simple power law scaling on η.

- No finite limit of the previous two forms exists. In this case the solution does not possess any similarity. One example is the non-rectifiable curve which is the graph of the function f defined by

$$f(x) = \begin{cases} x \sin \frac{1}{x}, & \text{if } x \in (0, 1], \\ 0, & \text{if } x = 0. \end{cases} \tag{1.23}$$

  The length L_η of the curve measured at a scale η goes to infinity when η goes to zero. However, the increase of L_η to infinity does not have any power-law scaling on η.

Self similar solutions of the first kind are everywhere in applied mathematics due to their relative simplicity to construct. These solutions not only are special exact solutions, but also can capture enormous important properties of the underlying equations. For the same equation, multiple self-similar solutions can

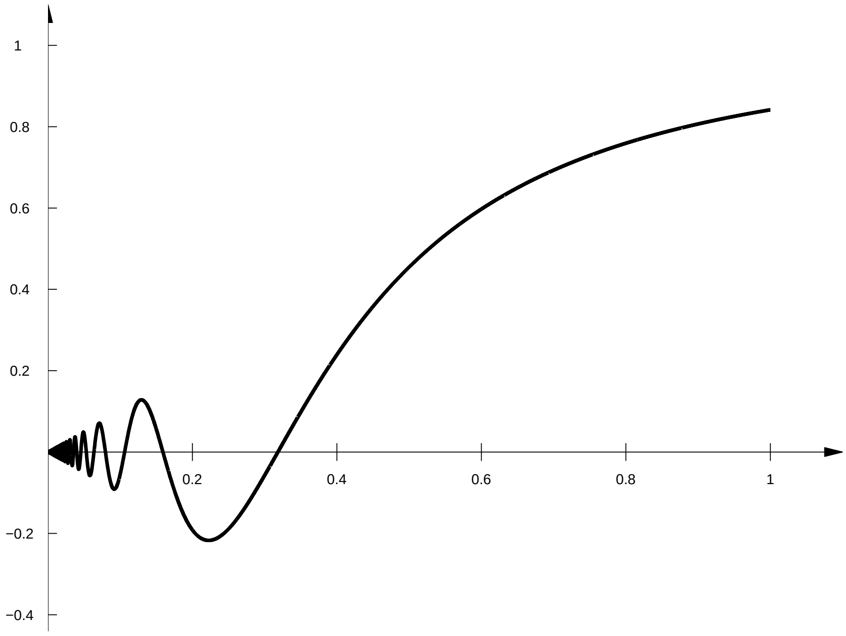

Figure 1.3: The non-rectifiable curve. The length increases as the length scale η decrease, but the increase does not any power law scaling on η.

exist, corresponding to different initial and boundary conditions. A few examples are listed below:

1. The fundamental solution to the Heat equation [Eva10]

$$u_t = \Delta u, \qquad x \in \mathbb{R}^n \tag{1.24}$$

   is

$$u(x,t) = (4\pi t)^{-n/2} \exp\left(-\frac{|x|^2}{4t}\right). \tag{1.25}$$

   When t goes to zero, it is the Green's function for the initial value problem, and when t goes to infinity, it captures the asymptotic behavior, in the sense that the solution to heat equation (1.24) with general initial condition converges to $M_0 u(x,t)$, where M_0 is the total(nonzero) mass of the initial data

$$M_0 = \int_{\mathbb{R}^n} u_0(x)dx = \int_{\mathbb{R}^n} u(x,t)dx.$$

When $M_0 = 0$, other self-similar solutions arise to characterize the long time asymptotic behavior. In one dimension, if the second moment (which is conserved)

$$M_2 = \int_{\mathbb{R}} x^2 u(x,t)$$

is nonzero, then the leading order behavior is governed by

$$t^{-3/2} H_1(xt^{-1/2}) \tag{1.26}$$

where H_1 is the Hermite function.

2. The Barenblatt solution with total mass M to the Porous Medium equation [Vaz07]

$$u_t = \Delta u^m, \qquad x \in \mathbb{R}^n \tag{1.27}$$

is

$$u(x,t) = t^{-\alpha}\left(C - \kappa x^2 t^{-2\alpha/n}\right)_+^{\frac{1}{m-1}}, \tag{1.28}$$

where

$$\alpha = \frac{n}{(m-1)n+2}, \qquad \kappa = \frac{(m-1)\alpha}{2mn}, \tag{1.29a}$$

and

$$M = a(m,n)C^\gamma, \quad \gamma = \frac{n}{2(m-1)\alpha} \tag{1.29b}$$

with some function a. It characterizes the long time behavior of solutions to initial data with compact support or decaying fast enough. It also characterizes the optimal regularity and other estimates to the solutions.

3. Traveling wave solution to the viscous Burgers equation [Bur74]

$$u_t + uu_x = \nu u_{xx} \tag{1.30}$$

is

$$u(x,t) = U_- + U_+ \tanh c(x - ct)/\nu, \tag{1.31}$$

where $U_- = u(-\infty, t)$, $U_+ = u(\infty, t)$ and the traveling speed $c = (U_- + U_+)/2$. Even though traveling wave solutions are not in the power-law scaling form as we have seen, they can be transformed into the desired form by introducing another set of variables $x = \ln y, t = \ln \tau$.

Self-similar solutions of the second kind, though even more ubiquitous in applied mathematics, are less known because of their analytical difficulties. In the following a few examples of self-similar solutions of the second kind and their *anomalous exponents* are listed.

1. The long time behavior of the filtration equation [BS69, KPV91, CW96]

$$u_t = \begin{cases} u_{xx}, & \text{if } u_{xx} > 0, \\ (1+\epsilon)u_{xx}, & \text{if } u_{xx} < 0. \end{cases} \tag{1.32}$$

   When $\epsilon = 0$ it is the heat equation and the long time asymptotics is exactly (1.25). When $\epsilon \neq 0$, the introduction of this dimensionless number ϵ changes the rate of decay and results in the solution of the form [BS69, CW96, KPV91]

$$u(x,t) = \frac{C}{t^\alpha} e^{-x^2/4t}, \tag{1.33}$$

   where α is a function of ϵ with $\alpha(0) = 1/2$.

2. The focusing problem for the Porous Medium equation [AG93, AA95]

$$u_t = \Delta u^m \tag{1.34}$$

   has a self-similar profile of the second kind. The numerical computation by Betelú, Aronson and Angenent [BAA00] in dimension two suggests a very rich dynamics of this problem under angular perturbation for different m.

3. Self-similar solution for the fast diffusion equation

$$u_t = \nabla \cdot (u^{-n} \nabla u), \quad 0 < n < 1, \tag{1.35}$$

with finite (but not conserved) mass is studied by Peletier and Zhang [PZ95].

4. Traveling wave solution to the Kolmogorov-Petrovskii-Piskunov [KPP37] (or Fisher [Fis37]) equation

$$u_t = u_{xx} + f(u) \tag{1.36}$$

of the form $u(x,t) = \theta(x - ct)$. In general, the traveling wave speed c can not be obtained explicitly, as in that for the Burgers equation, and phase plane analysis is used to find the qualitative and quantitative information.

1.2.3 Self-similarity in Finite Time Blowup Solutions of PDEs

Finite time blowup phenomena appear in many equations for physical models, including semilinear heat equations [GK85, FK92], nonlinear Schrödinger equations [Gla77, MPS86, FGW05], gravitational collapse [BW98] and pinch-off in surface diffusion [BBW98]. For a general review article, see [EF09]. Near the blowup time, it often happens that, because of the absence of any external scales, the solution collapses to the singularity in a self-similar way. Probably the most extensively studied one is the semilinear heat equation

$$u_t = \Delta u + f(u), \qquad f(u) = u^p \text{ or } f(u) = e^u \tag{1.37}$$

starting from 1960s in a seminar paper by Fujita [Fuj66]. However, it has been well-known since the 1970s that there is no exact self-similar solution of the form (for $f(u) = u^p$)

$$u(x,t) = (T-t)^{-1/(p-1)} U(x/(T-t)^{1/2}). \tag{1.38}$$

A refined analysis or center manifold theory close to the blowup time gives the following asymptotic form with a logarithm correction [Dol85, FK92, GK85, MZ97]

$$u(x,t) \sim \left(\frac{\beta}{T-t}\right)^{\beta}\left(1+\frac{p-1}{4p}\eta^2\right), \tag{1.39}$$

where

$$\eta = \frac{x}{\sqrt{[(T-t)|\ln(T-t)|}}, \quad \beta = \frac{1}{p-1}. \tag{1.40}$$

In contrast, quasilinear problems [SGK95, BG98]

$$u_t = (|u_x|^{\sigma} u_x)_x + e^u \quad \text{or} \quad u_t = (u^{\sigma} u_x)_x + u^p, \quad \sigma > 0 \tag{1.41}$$

or higher order parabolic equations [BGW04]

$$u_t = (-1)^{m+1} D_x^{2m} u + |u|^{p-1} u, \quad \text{or} \quad u_t = (-1)^{m+1} D_x^{2m} u + e^u \tag{1.42}$$

do possess exact self-similar blowup solutions, where D_x^{2m} is the 2m-th derivative with respect to x.

The nonlinear parabolic equation with a source

$$u_t = \nabla \cdot (u^{\sigma} \nabla u) + u^p, \quad t > 0, \ x \in \mathbb{R}^n, \tag{1.43a}$$

$$u(x,0) = u_0(x) \geq 0, \quad u_0^{\sigma+1} \in C^1(\mathbb{R}^n), \tag{1.43b}$$

contains many types of self-similar solutions, depending on the parameters σ and p. It is easy to see that the critical case is $p = \sigma + 1$. The behavior of the blowup solutions is substantially different in three cases in terms of the size of the blowup set [SGK95]:

1. When $p = \sigma + 1$, the solution goes to infinity on a set with nonzero measure.

2. When $1 < p < \sigma + 1$, the solution goes to infinity on the whole space.

3. When $p > \sigma + 1$, the solution goes to infinity only at discrete points.

Exact self-similar solutions of the first kind exist for any $p > 1$ and $\sigma > 0$ with above described behaviors. Even though these self-similar solutions arise only for special choices of initial data u_0, they characterize the behaviors of solutions, with general initial data, near the blowup time.

For those solutions with nontrivial blowup profiles, it is possible that the profiles match the exact analytical ones only near the core of the blowup point (or set), with deviation (though very small in magnitude) away from the core, sometimes called quasi-self-similar solutions. This is observed in the collapse of the cubic Nonlinear Schrodinger Equation, either for the Townes profile [CGT64, MPS86, MGF03] or for the ring profile [FGW05].

As we have seen, self-similar solutions possess a special position in the theory of partial differential equations. They can be the Green's function of the equation; they can capture the long time behavior of the solution; they can indicate the optimal regularity result since one can not expect to prove regularity more than that for the self-similar solution; they can used to classify the solutions in different parameter regime.

1.3 Outline of the Rest of the Thesis

After this brief introduction to the modeling of aggregation equation and background knowledge about self-similar solution in this chapter, the mathematical theory of the aggregation equation as well as the related blowup results are reviewed in Chapter Two. The blowup dynamics, in the context of self-similar solutions is studied in detail in the next two chapters, depending on the power γ in the homogeneous kernel $K(x) = |x|^\gamma$. When $\gamma \in (0, 2)$, the second-kind self-similar solutions are investigated both numerically and analytically in Chapter Three. When $\gamma \in (2, \infty)$, the solutions under the conventional similarity transform are studies in Chapter Four. This thesis is ended with a conclusion and possible extensions to many related future works.

CHAPTER 2

The Multidimensional Aggregation Equation

In this chapter, we review the basic mathematical theory for the aggregation equation

$$u_t = \nabla \cdot (u \nabla K * u), \tag{2.1}$$

starting from the elementary properties of the solutions to more advanced existence, uniqueness and regularity theory for both discrete and continuum problem. We pay special attention to the role of the kernels for different blowup behaviors. These qualitative blowup results are relevant to the special kernel $K(x) = |x|^\gamma$ in the following chapters, in which the detailed quantitative blowup behaviors are explored. Most of the results in this chapter are developed in [BB10, BCL09, Lau07] and also found in the review article [BL09].

2.1 Review of the Mathematical Theory of Aggregation Equation

2.1.1 Basic Properties of the Aggregation Equation

The aggregation equation (2.1) and its discrete analogue

$$\frac{d}{dt} x_i = -\sum_{j \neq i} m_j \nabla K(x_j - x_i) \tag{2.2}$$

have a lot of nice properties. These properties can be proved easily for smooth solutions but hold true for much more general solutions [Lau07].

- Conservation of the mass:

$$\int_{\mathbb{R}^n} u(x,t)dx = \int_{\mathbb{R}^n} u_0(x)dx. \tag{2.3}$$

  This is a direct consequence of the divergence structure of the equation.

- Conservation of the center of mass:

$$\int_{\mathbb{R}^n} xu(x,t)dx = \int_{\mathbb{R}^n} xu_0(x)dx. \tag{2.4}$$

  Taking the time derivative of the left hand side, we have

$$\begin{aligned}
\frac{d}{dt}\int_{\mathbb{R}^n} xu(x,t)dx &= \int_{\mathbb{R}^n} x\nabla\cdot(u\nabla K * u)dx \\
&= -\int_{\mathbb{R}^n} u(x,t)\nabla K * u(x,t)dx \\
&= -\int_{\mathbb{R}^n}\int_{\mathbb{R}^n} u(x,t)u(y,t)\nabla K(x-y)dxdy \\
&= -\int_{\mathbb{R}^n}\int_{\mathbb{R}^n} u(x,t)u(y,t)\nabla K(y-x)dxdy \quad \text{(switch } x \text{ and } y\text{)} \\
&= \int_{\mathbb{R}^n}\int_{\mathbb{R}^n} u(x,t)u(y,t)\nabla K(x-y)dxdy.
\end{aligned}$$

  In the last step the symmetry condition $K(x) = K(-x)$ is used. Therefore

$$\begin{aligned}
\frac{d}{dt}\int_{\mathbb{R}^n} xu(x,t)dx &= -\int_{\mathbb{R}^n}\int_{\mathbb{R}^n} u(x,t)u(y,t)\nabla K(x-y)dxdy \\
&= -\frac{d}{dt}\int_{\mathbb{R}^n} xu(x,t)dx, \qquad (2.5)
\end{aligned}$$

  which proves the conservation of the center of mass. If the initially the center of mass is not at the origin, we can always translate the coordinate system to make it at the origin. For this reason, in the rest of the thesis, we always assume the center of mass is at the origin, for both the discrete and continuum problem.

- Positivity preserving: If $u(x,0) = u_0(x) \geq 0$ then

$$u(x,t) \geq 0, \quad \text{for all } t > 0. \tag{2.6}$$

  This is proved by using the transport structure of the equation [Lau07].

- Non-increasing of the energy

$$E(u) = \frac{1}{2}\int_{\mathbb{R}^n}\int_{\mathbb{R}^n} K(x-y)u(x)u(y)dxdy. \tag{2.7}$$

  Taking the time derivative of the energy, we have

$$\begin{aligned}\frac{d}{dt}E(u) &= \int_{\mathbb{R}^n}\int_{\mathbb{R}^n} K(x-y)u_t(x)u(y)dxdy \\ &= -\int_{\mathbb{R}^n} u(x)|\nabla K * u(x)|^2 dx \\ &\leq 0. \end{aligned}\tag{2.8}$$

Remark 1. It is obvious that for the discrete particle system (2.2), the mass and center of mass is conserved and the discrete energy

$$E = \frac{1}{2}\sum_{i=1}^{L}\sum_{j\neq i} m_i m_j K(x_i - x_j) \tag{2.9}$$

is non-increasing.

2.1.2 Existence and Uniqueness for the Discrete Problem

For the discrete particle system (2.2) with symmetric kernel $K(x) = k(|x|)$ for some function k, the total mass $M = \sum_j m_j$ and the center of mass $c_M = (\sum_j x_j m_j)/M$ are conserved. Additional properties can be obtained with mild assumptions on the kernel K. One of the assumptions is the so called *Osgood condition*:

$$\int_0^1 \frac{dr}{k'(r)} = \infty, \tag{2.10}$$

which guarantees global existence of bounded solutions. On the other hand, when the Osgood condition is violated, i.e.

$$\int_0^1 \frac{dr}{k'(r)} < \infty, \tag{2.11}$$

then solutions blow up in finite time. In fact, the upper bound of this blowup time can be estimated with a monotonicity condition on $k'(r)/r$ shown below.

Denote by $R(t)$ the distance between the center of mass and the particle situated the furthest apart from the center of mass, i.e., $R(t) = |x_i(t) - c_M| = |x_i(t)|$ with i being its label. Thus, due to (2.2), we have

$$\frac{d}{dt}R(t)^2 = \frac{d}{dt}|x_i|^2 = -2\sum_{j\neq i} m_j \frac{(x_i - x_j)\cdot x_i}{|x_i - x_j|} k'(|x_i - x_j|)\,.$$

Since the ith particle is the one furthest away from the center of mass, we have that $(x_i - x_j)\cdot x_i \geq 0$ and that $|x_i - x_j| \leq 2R(t)$ for $j \neq i$. Assume that

$$\frac{k'(r)}{r} \text{ is non-increasing for } r > 0\,. \tag{2.12}$$

Putting together the previous information, we deduce

$$\frac{d}{dt}R(t)^2 \leq -\frac{k'(2R(t))}{R(t)} \sum_{j\neq i} m_j (x_i - x_j)\cdot x_i\,.$$

Due to conservation of mass and center of mass, we get

$$\sum_{j\neq i}(x_i - x_j)\cdot x_i m_j = \sum (x_i - x_j)\cdot x_i m_j = M|x_i|^2 = MR(t)^2,$$

and thus,

$$\frac{d}{dt}R(t) \leq -\frac{M}{2}\, k'(2R(t))\,. \tag{2.13}$$

If the potential $K(x) = k(|x|)$ satisfies the non-Osgood condition (2.11), then the ODE $dR/dt = -M\,k'(2R)/2$ with initial data $R = R_0$ touches down to zero in finite time, and therefore the particles aggregate in a single particle with the total mass M located at the center of mass before the touch-down time of the ODE (2.13), given by

$$T_B = \frac{2}{M}\int_0^{R_0} \frac{dR}{k'(2R)} = \frac{1}{M}\int_0^{2R_0} \frac{dR}{k'(R)}. \tag{2.14}$$

This bound is uniform for particles inside a fixed ball of radius R_0 initially with total mass M. This argument is inspired by and extends previous work in the control theory literature on cooperative motion with first order control laws involving pairwise interaction potentials (see [CHD07] for the case of attractive-repulsive potentials and [GP02] for quadratic potentials). The argument is proved rigorously in the following theorem:

Theorem 2.1.1 (Collapse of the ODEs [BCL09])**.** *Consider the ODE system* (1.3) *satisfying $k'(r)/r$ monotone decreasing, with $k''(r)$ defined and non-negative on* $(0, \infty)$*. If K satisfies the Osgood condition* (2.10) *then there exists a unique global-in-time forward solution with no collisions, in which the particles converge to their center of mass in infinite time. If K satisfies the non-Osgood condition* (2.11) *then there exists a unique global-in-time forward solution with collisions, in which the particles eventually all merge at their center of mass after finite time. In the latter case, for a given potential, an upper bound on the merger time is a function of the radius of support of the initial data and the total mass only.*

Remark 2. The particles can merge at different times and then into one at the final time.

Remark 3. If K satisfies the Osgood condition (2.10), the solution has backward uniqueness. Otherwise if K satisfies the non-Osgood condition (2.11), the solution does not have backward uniqueness.

In the next subsection we show how this collapsing support argument can be used to prove finite time blowup of the continuum problem in the case of non-

Osgood potentials. We consider bounded initial data, therefore the characteristic paths are smoother than the point particle case considered in this subsection. However we can still implement the estimate on the size of the support of the solution, proving finite time blowup of the continuum problem.

2.1.3 Local Existence Theory for the Continuum Problem

Let us first review the well-posedness of the continuum problem with bounded data. We build primarily on the work of [BB10, BCL09, Lau07]. These papers establish the existence and uniqueness theory for (1.1) in dimensions two and higher, in the case of an *acceptable* potential satisfying the following criteria:

Definition 2.1.1 ([Lau07])**.** The potential K on $\mathbb{R}^n$, $n \geq 2$ is *acceptable* if $\nabla K \in L^2(\mathbb{R}^n)$ and $\Delta K \in L^p(\mathbb{R}^n)$ for some $p \in [p^*, 2]$, where $\frac{1}{p^*} = \frac{1}{2} + \frac{1}{N}$. In the case of compactly supported initial data, we can take $\nabla K \in L^2_{\text{loc}}(\mathbb{R}^n)$ and $\Delta K \in L^p_{\text{loc}}(\mathbb{R}^n)$.

Remark 4. The properties of the *acceptable* kernels are needed in the proof of the local existence theory, using either successive approximations [Lau07] or mollifiers [BL07].

We note that the typical kernels considered satisfy the acceptability condition. In particular, the kernel $K(x) = 1 - e^{-|x|}$ is Lipschitz, satisfies ∇K bounded a.e. and thus is in $L^2_{\text{loc}}(\mathbb{R}^N)$. Moreover, the most singular case at the origin is $\Delta K \sim \frac{1}{|x|}$ which satisfies the L^p condition above in dimensions two and higher. The case of one space dimension has special issues and we discuss that at the end of this section.

The continuum model assumes a non-negative density $u(x, t)$ at position $x \in$

$\mathbb{R}^n$ and time $t > 0$ satisfying

$$\begin{cases} \dfrac{\partial u}{\partial t}(x,t) + \text{ div } [u(x,t)\vec{v}(x,t)] & = 0 & t > 0\,,\ x \in \mathbb{R}^n\,, \\ \text{with velocity field } \vec{v}(x,t) & := -\nabla K * u(x,t) & t > 0\,,\ x \in \mathbb{R}^N\,, \\ u(x,0) & = u_0(x) \geq 0 & x \in \mathbb{R}^n\,, \end{cases} \tag{2.15}$$

where $\vec{v}$ is the velocity field under which individuals in the swarm are moving obtained through the “averaging” of the pairwise potential by the distribution of mass.

We now review the well-posedness theory for H^s-solutions.

Theorem 2.1.2 (Existence theory for H^s data [BCL09, Lau07])**.** *Given initial data $u_0 \in H^s(\mathbb{R}^n)$, $n \geq 2$, for positive integer $s \geq 2$, there exists a unique weak solution $u(x,t)$ of* (2.15) *and a maximal interval of existence* $[0, T^*)$ *such that either $T^* = \infty$ or $\lim_{t\to T^*} \sup_{0\leq\tau\leq t} \|u(\cdot,\tau)\|_{L^q} = \infty$. The result holds for all $q \geq 2$ for $n > 2$ and $q > 2$ for $n = 2$.*

It is shown in [BCL09] that as long as the L^q-norm of the solution is bounded, then the H^s-norm of the solution must also remain bounded [BCL09, Proposition 2]. In other words, the L^q-norm controls the H^s-norm. This is why in the above theorem the eventual blow-up first occurs in L^q and it is in the same spirit of the Beale-Kato-Majda criteria [BKM84] for the breakdown of smooth solutions for 3-D Euler equations. The 3-D Euler equation can be written in the vorticity form

$$\boldsymbol{\omega}_t + \boldsymbol{u}\cdot\nabla\boldsymbol{\omega} = \boldsymbol{\omega}\cdot\nabla\boldsymbol{u}, \tag{2.16}$$

where $\boldsymbol{\omega}$ is the vector vorticity and the velocity $\boldsymbol{u}$ is determined from $\boldsymbol{\omega}$ by the relation

$$\boldsymbol{u} = -\nabla\times\Delta^{-1}\boldsymbol{\omega}. \tag{2.17}$$

The corresponding existence (or continuation) theory is that the $L^\infty(0,T;L^2)$ norm of the vorticity $\boldsymbol{\omega}$ is governed by the $L^1(0,T;L^\infty)$ norm of the vorticity. In other word, if the solution to (2.16) cannot be continued up to time T, then

$$\int_0^T \|\boldsymbol{\omega}(\cdot,t)\|_{L^\infty} dt = \infty. \tag{2.18}$$

When the kernel K is C^2, one can derive an a priori bound for u in L^∞ (see [TB04, Lau07]) thereby guaranteeing global existence of an H^s solution. Moreover, when the kernel has a Lipschitz point at the origin, for example the Morse potential $K(x) = 1 - e^{-|x|}$, one can have finite time blowup. The proof in [BCL09] uses the energy (2.8) and provides an *apriori* lower bound for E while simultaneously proving an *apriori* upper bound for the rate of decrease for the energy E when the data is radially symmetric and smooth. More recently these results have been extended in [BB10] to the case of solutions with (weaker) initial data in $L^1 \cap L^\infty$. With mild decay conditions at infinity and the same conditions on the kernel K as above, we have local in time well-posedness of the problem and continuation of solutions. For simplicity we state the result for data with compact support.

Theorem 2.1.3 (Existence theory for $L^1 \cap L^\infty$ data [BB10])**.** *Given compactly supported initial data $u_0 \in L^1(\mathbb{R}^n) \cap L^\infty(\mathbb{R}^n)$, $n \geq 2$, there exists a unique weak solution $u(x,t)$ of (2.15) and a maximal interval of existence $[0,T^*)$ such that either $T^* = \infty$ or $\lim_{t\to T^*} \sup_{0\leq\tau\leq t} \|u(\cdot,\tau)\|_{L^q} = \infty$. The result holds for all $q \geq 2$ for $n > 2$ and $q > 2$ for $n = 2$.*

Existence of solutions for $L^1 \cap L^\infty$ data is proved by constructing first the characteristics for the weak problem. This approach requires unique solutions to the characteristic equation, which requires a certain degree of regularity of the velocity field $\vec{v}$. Provided u is bounded, it is shown in [BB10] that $\vec{v}$ is Lipschitz continuous and moreover div$\vec{v}$ is log-Lipschitz continuous (Lipschitz continuous) in dimension two (three and higher).

Since the mass of the solution is conserved on its interval of existence, another way to prove finite time blowup is to derive an estimate for the size of the support of the solution. If an upper bound for the size of the support shrinks to zero in finite time, this also guarantees that the time interval of existence of the $L^1 \cap L^\infty$ solution is less than infinity. The analysis for the ODE case is extended to the continuum problem in the following theorem.

Proposition 2.1.4 (Frozen-in-time velocity estimate [BCL09])**.** *Assume $k'(r)/r$ is a monotone decreasing function of r. Consider a non-negative function $u : \mathbb{R}^n \to \mathbb{R}$ with total mass M, first moment zero and compact support. Consider any $B_R(0)$ containing the support of u. Then, for any $x \in \partial B_R(0)$ we have*

$$\vec{v}(x) \cdot x \leq -\frac{k'(2R)R}{2} M \leq 0,$$

where $\vec{v} = -\nabla K * u$.

The above proposition is now used to prove the following theorem. This is a generalization of [BL07, Theorem 6] and [BB10, Theorem 6.2] to the the case of less singular kernels satisfying (2.10) and the monotonicity conditions in Proposition 2.1.4. Also, significantly, the radial symmetry of the initial data, required in the proofs from [BL07, BB10] is no longer necessary.

Theorem 2.1.5 (Finite time blowup for compactly supported solution in L^∞ [BB10])**.** *Let u be a weak solution of* (2.15) *with non-negative compactly supported initial data in $L^\infty(\mathbb{R}^n)$. Let K satisfy the conditions* (2.11) *and $k'(r)/r$ monotone decreasing, $k'(r) > 0$. Then there exists a maximal time $T^* < \infty$ and a unique weak solution u to the problem* (2.15) *on the interval $[0, T^*)$. Moreover*

$$\lim_{t \to T^*} \sup_{0 \leq \tau \leq t} \|u(\cdot, \tau)\|_{L^q} = \infty \quad \text{for } q \in [2, \infty] \text{ if } n > 2 \text{ and } q \in (2, \infty] \text{ if } n = 2.$$

Proof. Given the existing continuation theorem, it suffices to prove that the solution ceases to exist in finite time. To do that, we prove a comparison principle for the support of the solution:

Proposition 2.1.6 (Comparison principle [BCL09])**.** *Let $\rho(x,t)$ be the weak solution in Theorem 2.1.5. Let $B_{R_0}(c_M)$ contain the support of the solution at time zero. Let $\tilde{R}(t)$ be the unique solution of the ordinary differential equation $dR/dt = -Mk'(2R)/2$. On any time interval of existence of the $L^1 \cap L^\infty(\mathbb{R}^N)$ solution $\rho(x,t)$, the support of ρ must lie inside $B_{\tilde{R}(t)}(c_M)$.*

2.1.4 Global Existence Theory for the Continuum Problem with Osgood Potential

In this section we review recent results for global existence of solutions in the case of Osgood potentials satisfying monotonicity conditions. To do this, we obtain refined estimates on the L^∞-norm of $\operatorname{div} \cdot \vec{v}$. We begin by reviewing the C^2 case, which has already been studied in the literature. Along characteristics, we have $\partial_t \rho + v \cdot \nabla \rho = -\rho \operatorname{div}(v)$, and this holds in the integral form [BB10], for the case of L^∞-weak solutions. Thus, by taking the L^∞-norm along all characteristics, we have a bound on the time evolution of $\|\rho\|_{L^\infty}$

$$\frac{d}{dt}\|\rho\|_{L^\infty} \leq \|\Delta K * \rho\|_{L^\infty} \|\rho\|_{L^\infty}. \tag{2.19}$$

In the case where K is C^2, we immediately get that

$$\|\Delta K * \rho\|_{L^\infty} \leq \|\Delta K\|_{L^\infty} \|\rho\|_{L^1},$$

which is a priori bounded and thus by Grönwall's lemma, gives a global bound for $\|\rho\|_{L^\infty}$. Combining this with the existence Theorem 2.1.7 provides the following result (the a priori bound has been proved in [BL07]):

Theorem 2.1.7 (Global-in-time solutions for C^2 potentials)**.** *Let K be an admissible C^2 kernel. Then the time and we have a global in time bound*

$$\|u(\cdot,t)\|_{L^\infty} \leq e^{Ct}\|u(\cdot,0)\|_{L^\infty},$$

where C depends on $\|\Delta K\|_{L^\infty}$ and the mass of u.

We also obtain the following corollary of the previous section:

Corollary 2.1.8 (Infinite time blow-up for C^2 potentials)**.** *Let K be an admissible C^2 kernel satisfying the the global-in-time weak solution of Theorem 2.1.7 has compact support, then it converges to a Dirac mass at the center of mass c_M as $t \to \infty$.*

We now show that the same result holds for potentials satisfying the weaker Osgood condition

$$\int_0^1 \frac{1}{k'(r)}dr = \infty.$$

Theorem 2.1.9 (Global-in time L^∞ and infinite time blow-up for Osgood potentials [BCL09])**.** *Assume $k''(r) > 0$ and that $k'(r)/r$ monotone decreasing in r. Then on the interval of existence $(0, T^*)$*

$$\frac{d}{dt}\|\rho\|_{L^\infty}^{-1/N} \geq -C(N,M)\,k'\left(M^{1/N}\|\rho\|_{L^\infty}^{-1/N}\right) \tag{2.20}$$

holds. As a consequence, if K satisfies the Osgood condition (2.10) *then for any compactly supported non-negative L^∞ solution of the aggregation equation stays bounded for all time and converges as $t \to \infty$ to a Dirac mass of size M located at its center of mass c_M.*

2.1.5 Well-posedness for Other Generalizations

In the previous subsections, only theory with the simplest form of the aggregation (1.1) is considered. This equation is extended to many situations, notably the inclusion of various diffusion effects, either degenerate or fractional. The existence and uniqueness of the aggregation with degenerate diffusion is considered by Bertozzi and Slepcev [BS10]; the local and global well-posedness is studied further by Bedrossian, Rodriguez and Bertozzi [BRB10].

On the other had, the aggregation equation with diffusion

$$u_t = \Delta u - \nabla \cdot (u \nabla K * u), \quad x \in \mathbb{R}^n,\ t > 0, \tag{2.21a}$$

$$u(x, 0) = u_0(x), \tag{2.21b}$$

is considered by Karch and Suzuki [KS10]. This variation of the aggregation equation includes the parabolic-elliptic Keller-Segel system

$$u_t = \nabla \cdot (\nabla u - u \nabla v), \quad x \in \mathbb{R}^n,\ t > 0, \tag{2.22a}$$

$$0 = \Delta v - \alpha v + u, \tag{2.22b}$$

as a special case in which the kernel K is given by a Bessel potential. Because of the strong smoothing effect of the diffusion, the regularity theory and the corresponding blowup/non-blowup results are obtained for much more general kernels K.

The same equation with fractional diffusion $-(-\Delta)^{\alpha/2}$ is considered by Li and Rodrigo [LR09]; depending on exponent α, the solution can blow in finite time for $\alpha \in (0, 1)$ or exists globally in time for $\alpha(1, 2)$.

2.2 Blowup Results for the Aggregation Equation

In the study of the regularity theory of the aggregation equation, the blowup phenomena attracted a lot of attentions. It is well-known that smooth solutions to nonlinear equations can develop singularity in finite time. This singularity can be the loss of smoothness or the blowup of the magnitude of the solution, as called the geometric mechanism or ODE mechanism in [Ali95]. The loss of regularity or geometric mechanism includes examples from system of conservation laws; the blowup of the magnitude of the solution or ODE mechanism includes nonlinear heat equations [QS07], nonlinear Schrödinger equation [SS99].

For the aggregation equation we consider here, the kernel is said to be *attractive* if $k'(r) \geq 0$. Any solutions corresponding to this kind of attractive kernel collapses, either finite time or infinite time, even though the initial data is smooth. When the solution is concentrated on a small spatial scale, only the leading non-constant order of the kernel K is relevant. For this reason, in the rest of the thesis, only the homogeneous kernel $K(x) = |x|^\gamma$ is considered. This special kernel is attractive and leads to aggregation only for $\gamma > 0$.

For the special case when $\gamma = 2$, thanks to the conservation of mass and center of mass, the original equation becomes linear and the solution is given by

$$u(x,t) = e^{2nMt} u_0(Xe^{2Mt}). \tag{2.23}$$

where M is the total mass and the center of mass c_M is assumed to be at the origin. Otherwise, according to the existence results reviewed above, the solutions blow up in finite time for $\gamma \in (0,2)$ and at infinite time for $\gamma \in (2,\infty)$, . Both situations are studied in details in the next two chapters. The special case $K(x) = |x|$ is studied in details by many authors, both analytically [BB10, Don10] and numerically [HB10].

2.2.1 Self-similar Solutions for $K(x) = |x|$

Examples of self-similar solutions for $K(x) = |x|$ are investigated [BB10]. In one dimension, there exist exact self-similar solutions of the form

$$u(x,t) = \frac{1}{T-t} U\left(\frac{x}{T-t}\right), \tag{2.24}$$

where U is supported on an interval. In higher dimensions, there exist Delta ring solutions of the form

$$u(x,t) = \sum_{i=0}^{L} m_j \delta(r - R_i(t)), \tag{2.25}$$

in which $\{R_i(t)\}$ is governed by the system of ODEs

$$\dot{R}_i(t) = -\sum_{j=0, j\neq i}^{L} m_j \psi(R_i(t), R_j(t)). \tag{2.26}$$

Here the function ψ is defined by

$$\begin{aligned} \psi(r,\rho) &= \frac{1}{\omega_N \rho^{N-1}} \int_{\partial B(0,\rho)} \nabla K(re_1 - y) \cdot e_1 d\sigma(y) \\ &= \frac{1}{\omega_N \rho^{N-1}} \int_{\partial B(0,\rho)} k'(|re_1 - y|) \frac{re_1 - y}{|re_1 - y|} d\sigma(y). \end{aligned} \tag{2.27}$$

These singular solutions, though exact, are unlikely evolved from smooth initial data. In fact, it is proved that

Theorem 2.2.1 (Non-existence of similarity solutions [BCL09])**.** *Let n be an odd space dimension larger than one and $K(x) = |x|$. Then there does not exist a non-negative similarity solution in $L^p(\mathbb{R}^n)$ for $p > 1$ whose support contains an open set.*

These self-similarity solutions of the first kind are further classified by Dong [Don10]:

Theorem 2.2.2. *Let $n \geq 3$ and $K(x) = |x|$. Then any radially symmetric first-kind similarity measure-valued solution is of the form*

$$\mu_t(x) = \frac{1}{R(t)} \hat{\mu}_0 \left(\frac{x}{R(t)} \right), \tag{2.28}$$

where

$$\hat{\mu}_0 = m_0 \delta_0 + m_1 \delta_{\rho_1} \tag{2.29}$$

for some constants $m_0, m_1 \geq 0$ and ρ_1.

Note that the singular measure-valued solutions described in Theorem 2.2.2 are not obtained in dynamic simulation of blowup for smooth initial data. However, there are related collapsing δ-ring solutions describing infinite time blowup for $\gamma > 2$. We show in Chapter 4 that after appropriate transformation, these solutions are attractors for smooth initial data.

CHAPTER 3

Finite-time Blowup: Self-similar Solution of the Second Kind

When $\gamma \in (0, 2)$, smooth solutions to the aggregation equation

$$u_t = \nabla \cdot (u \nabla K * u), \quad K(x) = |x|^\gamma \tag{3.1}$$

blows up in finite time according to the Osgood condition in [BCL09]. In this chapter, we discuss the details of the structure of the blowup using high resolution numerical simulations. We show that smooth radially symmetric solutions exhibit self-similar blowup solutions of the second kind. The nonexistence of smooth self-similar blowup solutions of the first kind is proved in some special cases, following by numerical schemes based on the method of characteristics. These *anomalous* exponents and their associated profiles in the special case of odd dimensions with the kernel $K(x) = |x|$ are calculated from an equivalent system of ODEs using shooting method. The asymptotic behavior when γ close to zero is also studied in the last section.

3.1 Self-similar Solutions of the Aggregation Equation

3.1.1 Similarity Analysis

First we introduce the following similarity variables y and τ

$$y = x(T-t)^{-\beta}, \quad \tau = -\ln(T-t), \tag{3.2}$$

and define a new function $U(y,\tau)$ such that

$$u(x,t) = (T-t)^{-\alpha} U(y,\tau), \tag{3.3}$$

where T is the blowup time, α and β are exponents characterizing the singularity when the blowup time is approached. We call the blowup dynamics self-similar if the transformed function U converges to some steady state as $t \to T^-$, or equivalently $\tau \to \infty$ for some appropriate constants α and β. When (3.3) is substituted into the original evolution equation for u, a routine calculation gives

$$\begin{aligned}
&(T-t)^{-\alpha-1}\left(\partial_\tau U + \alpha U + \beta y \cdot \nabla U\right) \\
&= (T-t)^{(n-2)\beta-2\alpha} \nabla_y \cdot \left(U(y,\tau) \nabla_y \int_{R^n} K\left((y-z)(T-t)^{\beta}\right) U(z,\tau) dz \right) \\
&= (T-t)^{(n+\gamma-2)\beta-2\alpha} \nabla_y \cdot (U \nabla_y K * U).
\end{aligned} \tag{3.4}$$

Given this, then the matching of the exponents of $(T-t)$ in equation (3.4) gives

$$\alpha = (n+\gamma-2)\beta + 1 \tag{3.5}$$

and the equation for U is

$$\partial_\tau U = \nabla \cdot (U \nabla K * U) - \alpha U - \beta y \cdot \nabla U. \tag{3.6}$$

Any exact self-similar profile U, if it exists, must satisfy the steady equation of (3.6), i.e.,

$$\nabla \cdot (U \nabla K * U) - \alpha U - \beta y \cdot \nabla U = 0, \tag{3.7a}$$

$$\nabla U|_{y=0} = 0, \quad \lim_{|y| \to \infty} U(y) = 0, \tag{3.7b}$$

where U has no explicit dependence on τ. To completely characterize the self-similar blowup dynamics, we need one extra condition to find the exponent β. Very often this kind of information can be readily available from a dimensional analysis or scale invariance of the underlying equation, like the parabolic scaling $\beta = 1/2$ for semilinear heat equation and Nonlinear Schrdinger equation, or $\beta = 1/(2m)$ for higher order parabolic equations as those in (1.42). Here, if the similarity solution concentrates mass in the core of the blowup, then $\alpha = n\beta$ from mass conservation, and consequently $\beta = 1$. However, numerical simulation of the blowup dynamics performed later shows that no mass is concentrated. In fact, it is proved analytically in [BCL09] that there is no such radially symmetric, self-similar solution in odd dimension larger than one, that concentrates mass. Taking $\alpha = n$, $\beta = 1$ in (3.7), we can integrate the equation in radial coordinate $r = |y|$,

$$-nU - rU_r = \frac{1}{r^{n-1}} \partial_r [r^{n-1} U \partial_r (K * U)].$$

Multiplying both sides with r^{n-1} and integrating once again, we get

$$-r^n U = r^{n-1} U \partial_r (K * U).$$

Assuming U is nonzero, we divide by $y^{n-1}U$ and integrate up again to get the final result,

$$-\frac{1}{2} r^2 + C = K * U. \tag{3.8}$$

Now we recognize that in odd dimension n larger than one, for the special case of $K = |x|$, applying repeated Laplacians to the right hand side of (3.8) gives

$\Delta^{(n-1)} K*U = c_n U$, whereas the left hand side gives $\Delta^{(n-1)}(y^2+C) = 0$. Hence we do not have a nontrivial exact similarity solution of first kind (conserving mass) in odd space dimension larger than one. A more rigorous analysis and derivation of this is discussed in Lagrangian coordinates in [BCL09]. In particular, that paper considers more general measure-valued similarity solutions due to the fact that there are easily constructed examples that concentrate mass in finite time in general space dimension, starting for initial data of the form of a delta-ring (support of the solution concentrated on the boundary of a sphere). However, here we consider solutions with U, a bounded function of spatial domain. Thus it is reasonable to look for similarity solutions of the second kind, for which α and β satisfy equation (3.5), which comes from the dimensional analysis of the dynamics, but may violate conservation of mass.

The nonlocal nature of the kernel $K * U$ presents a much more difficult problem, both analytically and numerically, compared to local problems as those from nonlinear diffusion equations and nonlinear Schrodinger equations. The usual techniques to tackle the equation for the self-similar profiles, like phase plane analysis and shooting methods, do not work here. Smooth self-similar blowup solutions in one dimension are considered by Bodnar and Velazquez [BV06] for different kernel potentials K. The technique used there is to introduce an auxiliary function

$$\psi(x,t) = \int_{-\infty}^{x} u(z,t)dz. \tag{3.9}$$

Moreover, for the special kernel $K = |x|$ considered here, the transformation (3.9) turns the equation (3.1) in one dimension into $\psi_t = \psi_x(2\psi - c)$ with $c = \psi(\infty, t) = \int_{-\infty}^{\infty} u_0(z)dz$, which is a constant. Another change of variable $\phi = c - 2\psi$ gives exactly the well-known inviscid Burgers equation $\phi_t + \phi\phi_x = 0$. For general initial condition, the finite time blowup of u is equivalent to the onset of shock of ϕ, with mass concentration and thus $\alpha = \beta = 1$ as considered in [BCL09]. However, for positive, even initial condition (the analogue for radially symmetric case in higher dimension), the blowup exhibits a different scaling. Let the self-similar blowup solution of ϕ be

$$\phi(x,t) = (T-t)^{\beta-\alpha} f(x(T-t)^{-\beta}), \tag{3.10}$$

Here the exponents are chosen such that $u = -\phi_x/2$ has the same form as (3.3). Similarly, we have $\alpha = 1$ and the equation for the profile

$$ff' + \beta y f' - (\beta - 1) f = 0. \tag{3.11}$$

Because of the L^∞-contraction of the solutions to Burgers equation, β must be equal to or greater than one. If $\beta = 1$, the only nontrivial solution is $f(y) = -y$, corresponding to the previous case. Otherwise if $\beta > 1$, we are looking for a power series expansion of f near the origin, i.e.,

$$f(y) = a_1 y + a_3 y^3 + a_5 y^5 + \cdots \tag{3.12}$$

The system of equations the coefficients must satisfy is

$$\begin{aligned} a_1^2 + a_1 &= 0 & & O(y) \\ 4a_1 a_3 + (2\beta+1) a_3 &= 0 & & O(y^3) \\ 6a_1 a_5 + 3a_3^2 + (4\beta+1) a_5 &= 0 & & O(y^5) \\ &\vdots \end{aligned} \tag{3.13}$$

If $a_1 = 0$, we have the trivial solution $f \equiv 0$. Therefore a_1 must be -1. For generic odd initial data, a_3 is nonzero, giving the exponent $\beta = 3/2$ and the coefficients of higher order terms are determined uniquely by a_3. Otherwise, β is decided from the next first nonvanishing term in the series.

Actually, we can directly integrate the equation (3.11) to get an implicit algebraic equation for f. Multiplying both sides of the differential equation (3.11) by $f(y)^{-(2\beta-1)/(\beta-1)}$ and taking the integration once, we get

$$f(y)^{-\frac{1}{\beta-1}}\left(1+\frac{y}{f(y)}\right)=c_1, \tag{3.14}$$

for some finite constant c_1. Since above equation holds in the limit when $y \to 0$, $f(y)$ must be $-y + o(y)$ such that $1 + y/f(y)$ vanishes at the origin. Applying the condition that the limit exist once more, we can find the next higher order term of $f(y)$ must be of the form

$$f(y) = -y + c_1(-y)^{\frac{\beta}{\beta-1}} + o\left((-y)^{\frac{\beta}{\beta-1}}\right). \tag{3.15}$$

Therefore, the exponent β is determined by the second non-vanishing term of the profile, which is ultimately determined by the initial condition. For generic even initial condition u_0, $f(y)$ is odd and the next non-vanishing term is cubic, giving $\beta/(\beta-1) = 3$, or $\beta = 3/2$. This *anomalous* exponent is consistent with the lower bound from numerical simulation in next section.

However, this special trick and these special solutions do not seem to carry over to higher dimensions. Unlike the nonlinear filtration problem, the exponents cannot be derived using perturbation [AV95] or renormalization group methods [GMO90] from known solutions in special cases or for some "unperturbed" problems. For this reason, high resolution numerical simulations are an important tool for uncovering the detailed dynamics of the blowup in higher dimensions.

3.1.2 Properties of the Self-similar Profile U

If the self-similar profile U exists, it must satisfy the steady state of (3.6)

$$\mathcal{A}U = \nabla\cdot(U\nabla K * U) - \alpha U - \beta y\cdot\nabla U = 0, \qquad K(x) = |x|^\gamma. \tag{3.16}$$

A few properties are immediately available. First there is a family of solutions: if U is a solution of (3.16), so is $U_\lambda(y) = \lambda^{n+\gamma-2}U(\lambda y)$ for any $\lambda > 0$. As a result, all the profiles U shown are normalized by the condition $U(0) = 1$. Moreove, this family of solutions gives an eigenpair for the the linearized operator $\mathcal{L}$ at U defined as

$$\mathcal{L}W = \nabla \cdot (U\nabla K * W)\nabla \cdot (W\nabla K * U) - \alpha W - \beta y \cdot \nabla W. \tag{3.17}$$

Using the invariance of the solution U_λ,

$$0 = \frac{d}{d\lambda}\mathcal{A}U_\lambda\bigg|_{\lambda=1} = \mathcal{L}\,\frac{d}{d\lambda}U_\lambda\bigg|_{\lambda=1} = \mathcal{L}\left[(n+\gamma-2)U + y\cdot\nabla U\right] \tag{3.18}$$

Using this eigenfunction $e_1(y) = (n+\gamma-2)U + y\nabla U$ of the zero eigenvalue of $\mathcal{L}$, the steady state equation (3.16) and the relation (3.5), we can get

$$\mathcal{L}\left[\alpha U + \beta y\cdot\nabla U\right] = \mathcal{L}(U) = \alpha U + \beta y \cdot \nabla U, \tag{3.19}$$

where $e_2 = \alpha U + \beta y \cdot \nabla U$ is the eigenfunction. This eigenpair is related to the time translation of the solution $u(x,t) = (T-t)^{-\alpha}U(x(T-t)^{-\beta})$. In other words, if the time t is translated to $t+\epsilon$ or

$$T - t - \epsilon = (T-t)(1-\epsilon e^\tau) \tag{3.20}$$

then

$$\begin{aligned} u^\epsilon(x,t) &= (T-t-\epsilon)^{-\alpha}U(x(T-t-\epsilon)^{-\beta}) \\ &= (T-t)^{-\alpha}(1-\epsilon e^\tau)^{-\alpha}U(x(T-t)^{-\beta}(1-\epsilon e^\tau)^{-\beta}) \\ &= u(x,t) + \epsilon e_2(x(T-t)^{-\beta}(1-\epsilon e^\tau)^{-\beta}) + O(\epsilon^2). \end{aligned} \tag{3.21}$$

Even though the eigenvalue associated with v_1 is positive, the blowup profile is stable; any perturbation in this mode results in a translation in the blowup time. However, this mode does prevent any direct computation of the profile U from (3.6); we have to either evolve the solution near the blowup time or compute the some rescaled solution (the Renormalization Group Method), as shown in the next section.

Another numerical observed property is the rate of the algegraic decay of the radially symmetric solution, i.e.

$$U(y) \sim |y|^{-\alpha/\beta} = |y|^{-(n+\gamma-2)-\frac{1}{\beta}}. \tag{3.22}$$

In other words, the leading order asymptotics of the solution in the far field is governed by

$$\alpha U + \beta y \cdot \nabla U \tag{3.23}$$

in (3.16) and is a direct consequence of spatial and temporal interaction only, but not the part associated with the nonlocal convection. Another consequence of this algebraic decay is the existence of an "envelope" of the solution away from the origin, when the blowup time is approached.

3.2 Numerical Computation of the Blowup Dynamics

3.2.1 The Method of Characteristics in General Dimension

The computation of blowup solutions is usually quite challenging, due to the small scale of the blowup set, which cannot be resolved quite well by conventional numerical schemes. One of the most popular schemes is the Moving Mesh Method [BHR96, BCR05, HMR08], using an equipartition principle to give a separate equation for the mesh, to concentrate the computation on those regions where high resolution is desired. Another one is dynamic rescaling used in Nonlinear Schrodinger Equations ([MPS86] and [FGW05]). However, most of these schemes require a knowledge of those exponents characterizing the blowup to capture the dynamics accurately. Therefore they tend to work more successfully for self-similar solutions of the first kind.

Here we take advantage of the fact that our problem is a first order conservation law and thus we can use the method of characteristics to solve two coupled ODEs, one for the radial position r and the other for the solution u. In radial coordinates, the original equation can be written as

$$u_t = \frac{\partial u}{\partial r}\frac{\partial}{\partial r}K * u + u\Delta_r K * u, \tag{3.24}$$

where $\Delta_r = \partial_{rr} + \frac{n-1}{r}\partial_r$. The system of ODEs along the characteristics is thus

$$\frac{dr}{dt} = -\frac{\partial}{\partial r}K * u, \quad \frac{du}{dt} = u\Delta_r K * u. \tag{3.25}$$

The method of characteristics is used in many of the analytical arguments to prove the existence and other important properties of the aggregation equation (1), see [BV06] and [BB10]. This method provides a natural adaptive grid scheme to concentrate spatial resolution near the blowup point or set, and was employed to investigate gravitational collapse by Brenner and Witelski [BW98]. Moreover, for nonnegative initial data, we have the monotonicity condition $\frac{\partial}{\partial r}K * u \geq 0, \Delta_r K * u > 0$, i.e., the points always move towards to the origin and the magnitude is always increasing along the path. Thus our scheme preserves the positivity of the solution. The numerical results indicate that this simple scheme resolves the profiles quite well, both near the core and far away from it. If the self-similarity were of the first kind, then the characteristics would exactly preserve the spatial resolution going into the blowup. Since it is a second-kind similarity solution with anomalous scaling (i.e., the characteristics do not scale in time as the similarity variable) we lose resolution over time, but at a relatively slow rate compared with the dynamics of blowup.

The system (3.25) is solved using the conventional fourth order Runge-Kutta method, with the size of the time step Δt adapted according to the following two criteria: (a) The relative increase of the solution at all points is bounded by a threshold at each time step. (b) The nodes cannot cross each other during each time step. Finally, we need to compute the convolution of the kernel. We first give a general formulation for any dimension greater than two and then a special one in odd dimensions three and higher, to reduce computational effort by one order of magnitude.

Instead of calculating $K * u$ once and taking the numerical derivatives to solve (3.25), we find $\frac{\partial}{\partial r} K * u$ and $\Delta_r K * u$ directly by computing the derivatives of the kernel, i.e.,

$$\frac{\partial}{\partial r} K * u = c_n \gamma \int_0^\infty u(r') r'^{n-1} K_1(r, r') d\theta dr', \tag{3.26a}$$

$$\Delta_r K * u = \gamma(n + \gamma - 2) c_n \int_0^\infty u(r') r'^{n-1} K_2(r, r') dr', \tag{3.26b}$$

where

$$K_1(r, r') = \int_0^\pi (r - r' \cos\theta)(r^2 + r'^2 - 2rr' \cos\theta)^{\gamma/2-1} \sin^{n-2}\theta, \tag{3.27a}$$

$$K_2(r, r') = \int_0^\pi (r^2 + r'^2 - 2rr' \cos\theta)^{\gamma/2-1} \sin^{n-2}\theta d\theta, \tag{3.27b}$$

where c_n is the volume of the unit sphere in R^{n-1}. The computation can still be expensive, because at each point we have to perform a double integration. The expense can be reduced by observing the homogeneity of the kernel, which gives the following formulation

$$\begin{aligned} &(r - r' \cos\theta)(r^2 + r'^2 - 2rr' \cos\theta)^{\gamma/2-1} \\ &= \begin{cases} \max(r, r')^{\gamma-1}(1 - \rho \sin\theta)(1 + \rho^2 - 2\rho \sin\theta)^{\gamma/2-1}, & \text{if } r' \le r, \\ \max(r, r')^{\gamma-1}(\rho - \sin\theta)(1 + \rho^2 - 2\rho \sin\theta)^{\gamma/2-1}, & \text{if } r \le r', \end{cases} \end{aligned} \tag{3.28a}$$

$$(r^2 + r'^2 - 2rr' \cos\theta)^{\gamma/2-1} = \max(r, r')^{\gamma-2}(1 + \rho^2 - 2\rho \sin\theta)^{\gamma/2-1}, \tag{3.28b}$$

where $\rho = \min(r, r')/\max(r, r')$. In this way, the integrations of the kernel with respect to the angular variable have only to be calculated once at the very beginning as functions of $\rho \in [0, 1]$, i.e., we only need to perform numerical integrations once for the auxiliary functions

$$I_1(\rho) = \int_0^{\pi} (1 - \rho\cos\theta)(1 + \rho^2 - 2\rho\sin\theta)^{\gamma/2-1} \sin^{n-2}\theta d\theta, \tag{3.29a}$$

$$I_2(\rho) = \int_0^{\pi} (\rho - \cos\theta)(1 + \rho^2 - 2\rho\sin\theta)^{\gamma/2-1} \sin^{n-2}\theta d\theta, \tag{3.29b}$$

$$I_3(\rho) = \int_0^{\pi} (1 + \rho^2 - 2\rho\sin\theta)^{\gamma/2-1} \sin^{n-2}\theta d\theta. \tag{3.29c}$$

The auxiliary variable ρ is chosen such that those integrations are computed only at discrete points and the interpolations of I_1, I_2 and I_3 are restricted on the bounded interval $[0,\ 1]$. Therefore these functions I_1, I_2 and I_3 can be computed as accurately as needed without increasing the computation effort during the time evolution. In this way the total computational expense is reduced to $O(N^2)$ at each time step, where N is number of spatial points used to represent the solution. These auxiliary functions (Figure 3.1 for $\gamma = 1$ and Figure 3.2 for $\gamma = 0.4$) are relatively smooth inside the interval $[0, 1]$ for dimension greater or equal than three, but not at $\rho = 1$ if γ is small in lower dimensions. It is easy to see that $I_3(1)$ actually becomes divergent as the dimension n less or equal than two. For these reason, the computations are performed only for $n > 2$.

3.2.2 Computation Reduction for the Special Kernel $K(x) = |x|$ in Odd Dimensions

In odd dimension, using the fact that the successive Laplacians of the kernel $K(x) = |x|$ is proportional to the fundamental solution of the Laplace equation, we can further reduce the computation to be $O(N)$ per time step. This is exactly the fact used to prove the nonexistence of mass concentrating self-similar solutions

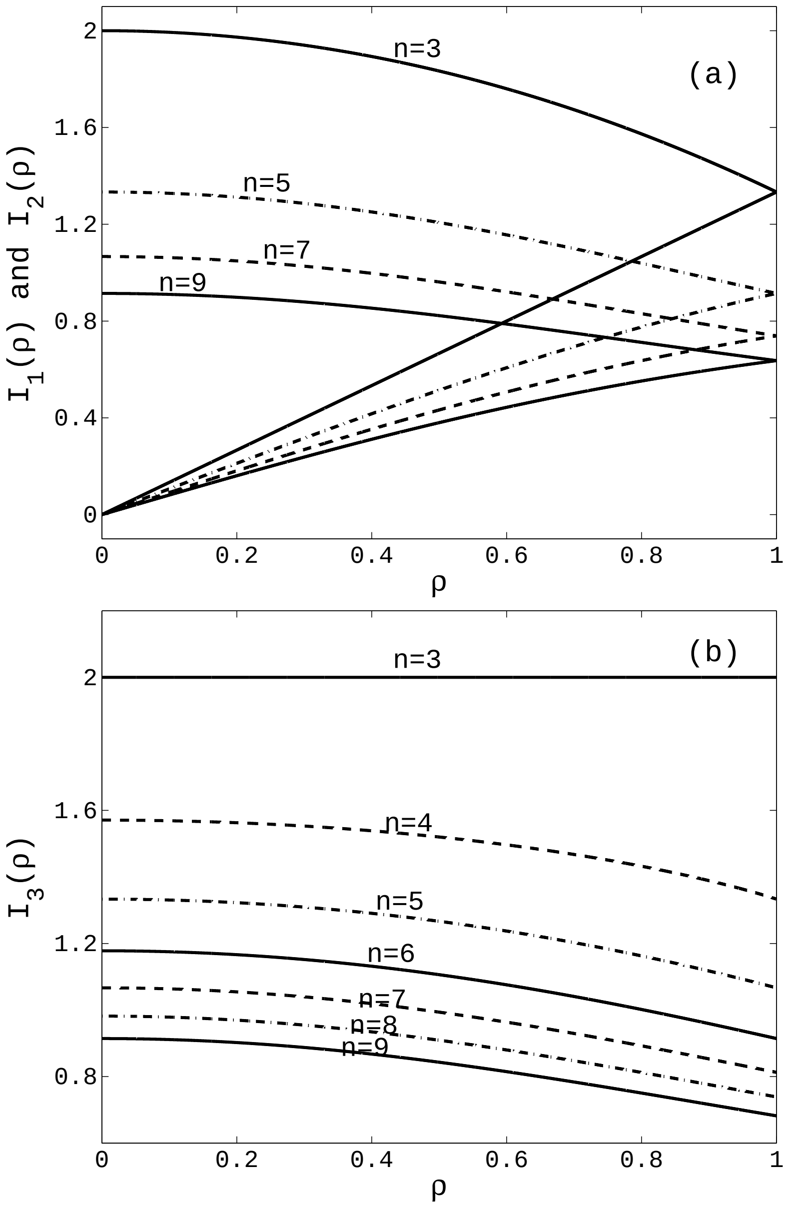

Figure 3.1: Auxiliary functions in different spatial dimensions for $\gamma = 1$: (a) I_1 (upper branch) and I_2 (lower branch), (b) I_3.

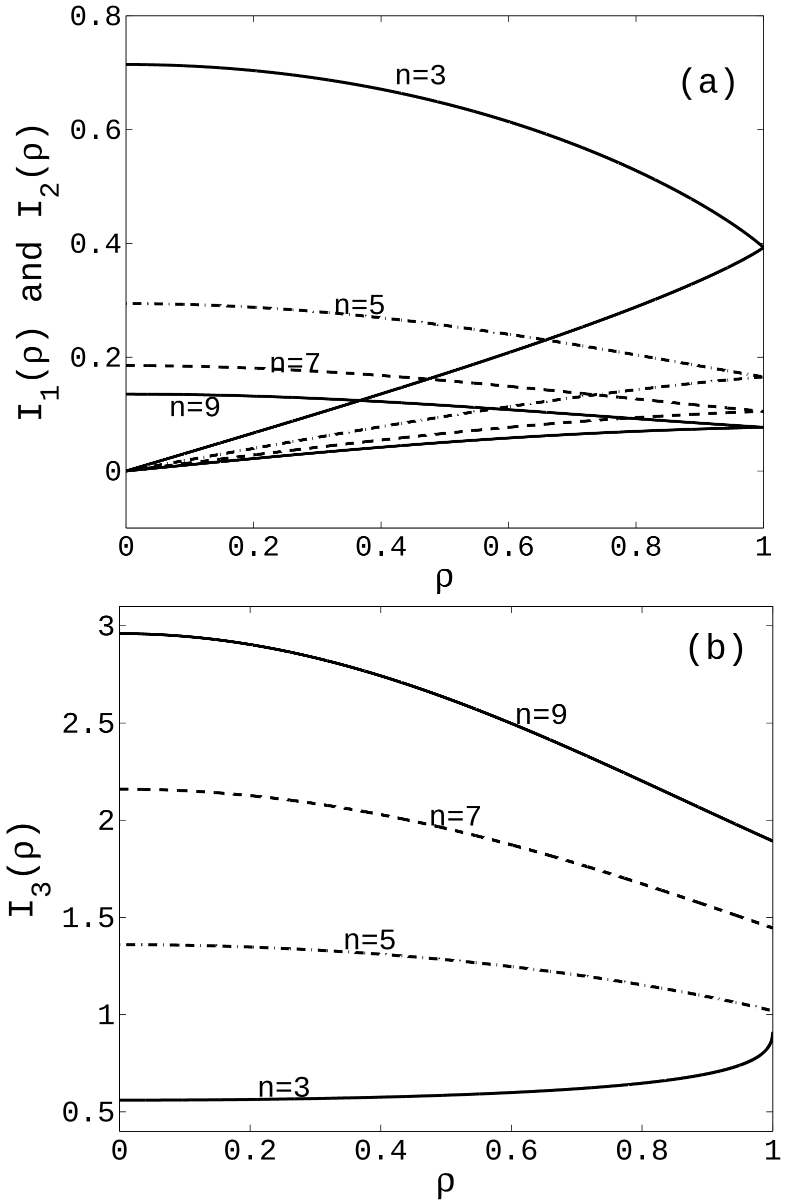

Figure 3.2: Auxiliary functions in different spatial dimensions for $\gamma = 0.4$: (a) I_1 (upper branch) and I_2 (lower branch), (b) I_3. For the smaller γ here, $I_3(\rho)$ is not smooth at $\rho = 1$ in dimension three, which may introduce numerical artifacts.

in [BCL09]. First, we start with dimension three to give the basic idea and then generalize it to any odd dimension greater than three. Let $v_0 = u$, and define v_1 and v_2 to be the solutions of the following equations

$$-\Delta v_1 = v_0, \quad \Delta v_2 = 8\pi v_1 \quad \text{ in } R^3, \tag{3.30}$$

with v_1 and v_2 decay to zero at infinity. We can just write down the solution via the method of fundamental solution, i.e.,

$$\begin{aligned} v_1(x) &= \int_{R^3} \frac{v_0(y)}{4\pi|x-y|}dy, \\ v_2(x) &= \int_{R^3} \frac{2v_1(y)}{|x-y|}dy = \int_{R^3}\int_{R^3} \frac{v_0(z)}{2\pi|x-y||y-z|}dzdy \\ &= \int_{R^3} |x-z|u(z)dz = K * u(x). \end{aligned} \tag{3.31}$$

In the radial symmetric case, we only need to solve

$$-\frac{1}{r^2}\frac{d}{dr}\left(r^2\frac{dv_1}{dr}\right) = v_0, \quad -\frac{1}{r^2}\frac{d}{dr}(r^2 v_{2r}) = 8\pi v_1, \tag{3.32}$$

with the following boundary condition

$$v_1(\infty) = 0, \quad \frac{\partial v_1(0)}{\partial r} = 0, \quad v_{2r}(0) = 0. \tag{3.33}$$

Then the right hand sides of the equations in (3.25) are replaced by

$$\frac{\partial}{\partial r}K * u = -v_{2r}, \quad \Delta_r K * u = 8\pi v_1, \tag{3.34}$$

with the time scaled by 8π. Note that we only need to find the derivative $\partial_r v_2$ of v_2, instead of v_2 itself. In actual implementation, the infinity boundary condition $v_1(\infty) = 0$ is transformed to a condition at $r = 0$, i.e., the value of $v_1(0)$,

$$v_1(0) = -\int_0^\infty \frac{\partial v_1(r)}{\partial r}dr = \int_0^\infty \frac{1}{r^2}\int_0^r v_0(s)s^2 ds dr = \int_0^\infty u(r)r dr. \tag{3.35}$$

This integral is usually truncated on a bounded domain if u is compactly supported or decays fast enough. In theory, this transformed boundary condition at the origin gives the unique zero boundary condition at infinity, while any inappropriate choice of v_1 at the end of the computational domain (an approximation to the condition $v_1(\infty) = 0$) could give a different effective kernel K, resulting in some inconsistence in theory and numerics. Once we have the right boundary condition, we can use an $O(N)$ numerical quadrature scheme to find the solution of (3.32), i.e.,

$$v_1(r) = v_1(0) - \int_0^r \frac{1}{\eta^2} \int_0^\eta u(s)s^2 ds d\tau = v_1(0) - \int_0^r u(s)(s - \frac{s^2}{r})ds, \tag{3.36a}$$

$$v_{2r}(r) = \frac{8\pi}{r^2} \int_0^r v_1(s)s^2 ds. \tag{3.36b}$$

In odd dimension greater than three, with $n = 2k + 1$, similarly we introduce $v_1, v_2, \cdots, v_{k+1}$ such that

$$-\Delta v_1 = v_0,\ -\Delta v_2 = v_1,\ \cdots,\ -\Delta v_k = v_{k-1},\ \Delta v_{k+1} = d_k v_k \quad \text{in } R^n, \tag{3.37}$$

and finally set in the characteristics ODEs (3.25)

$$\frac{\partial}{\partial r} K * u = -\frac{\partial v_{k+1}}{\partial r}, \quad \Delta_r K * u = d_k v_k, \tag{3.38}$$

where $v_0 = u$ and

$$d_k = 2^k(2k+1)k! \frac{\pi^{\frac{2k+1}{2}}}{\Gamma(k+1+\frac{1}{2})}. \tag{3.39}$$

To transform the boundary condition at infinity to the one at the original, we need to find the appropriate integration like (3.35) with the aid of fundamental solution of the Laplace equation, which is given by

$$N(x) = \frac{1}{n(n-2)\omega_n |x|^{n-2}}, \quad \omega_n = \frac{\pi^{n/2}}{\Gamma(n/2+1)}, \tag{3.40}$$

where ω_n is the volume of the unit sphere in R^n. Using the presentation formula of the solution to the Poisson equation, we have

$$v_i(x_i) = \int_{R^n} \cdots \int_{R^n} N(x_i - x_{i-1})N(x_{i-1} - x_{i-2}) \cdots N(x_1 - x_0)u(x_0)dx_0 dx_1 \cdots dx_{i-1} \tag{3.41}$$

for any $1 \leq i \leq k+1$. Translation and rotation invariance of the fundamental solutions gives the following identity

$$\int_{R^n} \cdots \int_{R^n} N(x_i - x_{i-1}) N(x_{i-1} - x_{i-2}) \cdots N(x_1 - x_0) dx_1 \cdots dx_{i-1} = N_i(x_i - x_0), \tag{3.42}$$

for some radially symmetric function N_i. Moreover, dimensional analysis indicates that N_i is homogeneous of degree $2i - n$, i.e.,

$$N_i(x_i - x_0) = \frac{c_{i,n}}{n\omega_n} |x_i - x_0|^{2i-n} \tag{3.43}$$

for some constant $c_{i,n}$. When $i = 1$, this is just the fundamental solution, giving the following initial condition

$$c_{1,n} = \frac{1}{n-2}. \tag{3.44}$$

We can find a recursive relation for $c_{i,n}$ by taking the negative Laplacian of N_i w.r.t x_i. Formally, on one hand using equation (3.43),

$$-\Delta_{x_i} N_i(x_i - x_0) = \frac{2(n-2i)(i-1)c_{i,n}}{n\omega_n} |x_i - x_0|^{2(i-1)-N}. \tag{3.45}$$

On the other hand, using the definition of N_i,

$$\begin{aligned}
& -\Delta_{x_i} \int_{R^n} \cdots \int_{R^n} N(x_i - x_{i-1}) N(x_{i-1} - x_{i-2}) \cdots N(x_1 - x_0) dx_1 \cdots dx_{i-1} \\
= & \int_{R^n} \cdots \int_{R^n} \delta(x_i - x_{i-1}) N(x_{i-1} - x_{i-2}) \cdots N(x_1 - x_0) dx_1 \cdots dx_{i-1} \\
= & \int_{R^n} \cdots \int_{R^n} N(x_i - x_{i-2}) \cdots N(x_1 - x_0) dx_1 \cdots dx_{i-2} \\
= & \frac{c_{i-1,n}}{n\omega_n} |x_i - x_0|^{2(i-1)-N}.
\end{aligned} \tag{3.46}$$

Match the coefficients of above two identities, we have the following recursive formula

$$c_{i,n} = \frac{1}{2(i-1)(n-2i)} c_{i-1,n} \tag{3.47}$$

and consequently with the initial condition (3.44),

$$c_{i,n} = \frac{1}{2^{i-1}(i-1)!(n-2i)!!}, \tag{3.48}$$

where $m!!$ is the double factorial of m. Finally, we get the boundary condition of v_i at the origin in terms of the integral with u, i.e.,

$$v_i(0) = \frac{c_{i,n}}{n\omega_n} \int_{R^n} |x_0|^{2i-n} u(x_0) dx_0 = \frac{1}{2^{i-1}(i-1)!(n-2i)!!} \int_0^\infty r^{2i-1} u(r) dr. \tag{3.49}$$

With these boundary conditions, we can find all the auxiliary functions v_is through a series of $O(N)$ numerical integrations like (3.36) to find the right hand side the characteristic ODEs (3.25).

3.2.3 Postprocessing of the Numerical Data

Close to the blowup time, $U(0,\tau)$ should approach a constant U_0, and $u(0,t) \approx (T-t)^{-\alpha} U_0$. The time derivative $u_t(0,t)$ can be approximated by $u(0,t)$ too, i.e.,

$$u_t(0,t) \sim \alpha U_0^{-1/\alpha} u(0,t)^{1+1/\alpha}. \tag{3.50}$$

On the other hand, from the second characteristic ODE (3.25), $u_t(0,t) = u(0,t)\Delta_r K * u(0,t)$, we have

$$\ln\left(\Delta_r K * u(0,t)\right) = \ln(\alpha U_0^{-1/\alpha}) + \frac{1}{\alpha} \ln u(0,t). \tag{3.51}$$

Using $u(0,t), \Delta_r K * u(0,t)$ at each time step, a simple least square fitting gives the pair of parameters (α, U_0), as in Figure 3.3(a). To estimate the exponent β for spatial spread, we need to introduce a spatial scale. The most natural one is the half-width of the blowup profile, $r_{1/2}(t)$, the position at which the magnitude is half of that at the origin, i.e.,

$$u(r_{1/2}(t), t) = u(0,t)/2. \tag{3.52}$$

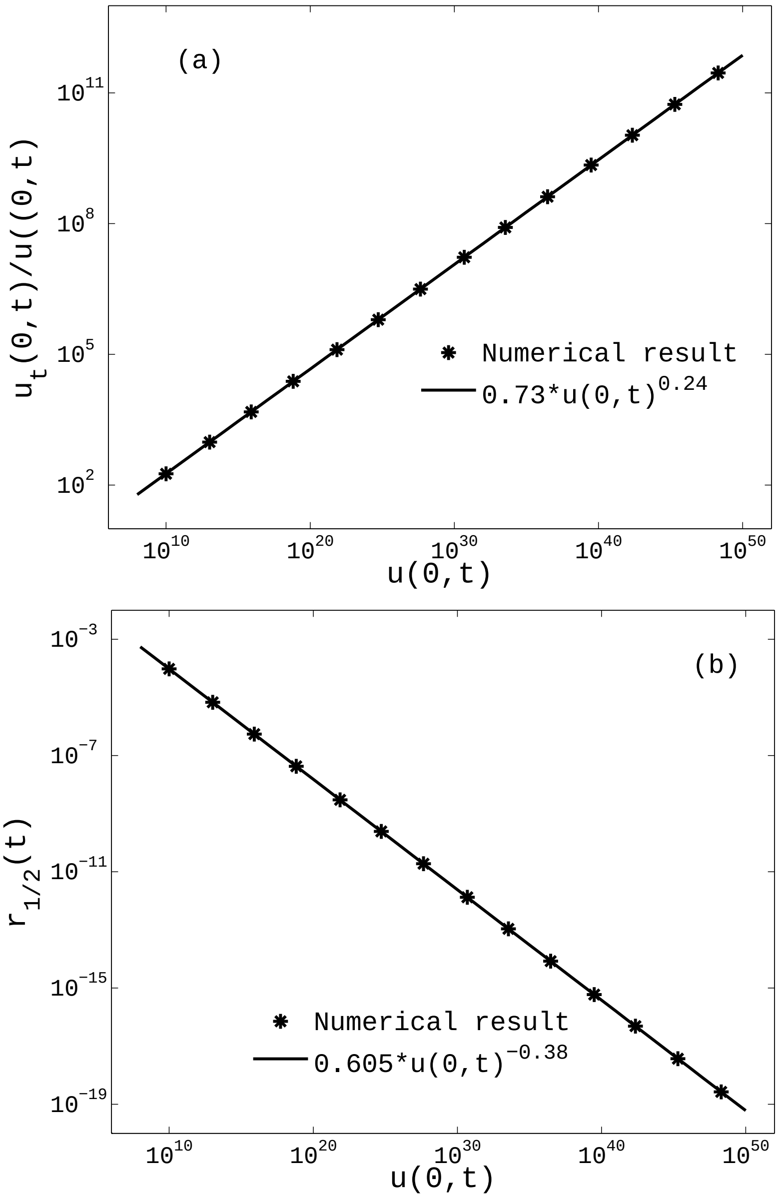

Figure 3.3: Estimation of α and β in dimension three for $\gamma = 1$. The straight lines in the log-log plots indicate a strong evidence of the self-similar blowup of the radially symmetric solutions.

The similarity form of the blowup implies

$$r_{1/2}(t) \sim r_0(T-t)^{\beta} \tag{3.53}$$

for some constant r_0. Using $r_{1/2}(t)$ (from interpolation if there is no function value that is exactly half of the maximum magnitude) and $T-t$ estimated with parameters obtained above, we can get β, as in Figure 3.3(b). In all the parameter estimation, only those data that close to blowup time ($u(0,t) > 10^{10}$) is used and the profiles should be radially decreasing such that there is one unique $r_{1/2}(t)$. The simulation is terminated when $u(0,t)$ reaches an upper bound 10^{50} provided that the profile near the origin is well resolved, say there are at least one hundred points nodes on the interval $[0, r_{1/2}(t)]$.

3.2.4 Numerical Renormalization Group Method

Since we are more interested in the exponents characterizing the intermediate asymptotics of the dynamics than other quantitative details, we can rescale the solution appropriately to get the the profile. This is the basic principle underlying Renormalization Group Method, which is employed successfully to the numerical investigation of nonlinear filtration and porous medium equations [CG95, BAA00].

We start with the solution $u^{(0)}(x,t) = u(x,t)$, whose solution is known on the time interval $[t_0^0, t_1^0]$. Without loss of generality, we let $u^{(0)}(0, t_0^0) = 1$ and t_1^0 is determined implicitly by $u^{(0)}(0, t_1^0) = M$ for some predetermined constant $M > 1$. For a given guess of the exponent β_m, at then end of $m-$th iteration, we can renormalize the function as

$$u^{(m+1)}(x, t_0^{m+1}) = M^{-1} u^{(m)}(xM^{-\beta_m/\alpha_m}, t_1^m), \qquad \alpha_m = (n-1)\beta_m + 1. \tag{3.54}$$

An equation for β_m can be estimated from the spatial-temporal relation of the blowup dynamics. Near blow-up time, we have

$$u(0,t) = (T-t)^{-\alpha} U_0, \qquad r_{1/2}(t) = (T-t)^{\beta} r_0, \tag{3.55}$$

where $r_{1/2}(t)$ is the position where u is half of u at the origin, i.e.,

$$u(r_{1/2}(t), t) = \frac{1}{2} u(0,t). \tag{3.56}$$

Therefore, on one hand we have

$$\frac{d \ln u(0,t)}{d \ln r_{1/2}(t)} = \frac{d \ln u(0,t)/dt}{d \ln r_{1/2}(t)/dt} = -\frac{\alpha}{\beta} = 1 - n - \frac{1}{\beta}. \tag{3.57}$$

On the other hand, using the original evolution equation, we can calculate the time derivatives explicitly, i.e.,

$$\frac{d \ln u(0,t)}{d \ln r_{1/2}(t)} = \frac{r_{1/2}(t)}{u(0,t)} \frac{du(0,t)/dt}{dr_{1/2}(t)/dt} = \frac{r_{1/2}(t)}{u(0,t)} \frac{\nabla \cdot (u \nabla K * u)|_{r=0}}{dr_{1/2}(t)/dt}. \tag{3.58}$$

Finally $dr_{1/2}(t)/dt$ can be obtained by taking the time derivative of equation (3.56)

$$u_r(r_{1/2}(t), t) \frac{dr_{1/2}(t)}{dt} + u_t(r_{1/2}(t), t) = \frac{1}{2} u_t(0,t), \tag{3.59}$$

or equivalently

$$\frac{dr_{1/2}(t)}{dt} = \frac{\frac{1}{2} \nabla \cdot (u \nabla K * u)|_{r=0} - \nabla \cdot (u \nabla K * u)|_{r=r_{1/2}(t)}}{u_r(r_{1/2}(t), t)}. \tag{3.60}$$

At the end of $m-$th iteration, the exponent β_m is solved by combining (3.57) and (3.58), i.e.,

$$1 - n - \frac{1}{\beta_m} = \frac{r_{1/2}(t_1^m)}{u^{(m)}(0, t_1^m)} \frac{A_m}{B_m}, \tag{3.61}$$

where

$$A_m = u_r^{(m)}(r_{1/2}(t_1^m), t_1^m) \nabla \cdot (u^{(m)} \nabla K * u^{(m)})|_{r=0} \tag{3.62a}$$

$$B_m = \frac{1}{2} \nabla \cdot (u^{(m)} \nabla K * u^{(m)})|_{r=0} - \nabla \cdot (u^{(m)} \nabla K * u^{(m)})|_{r=r_{1/2}(t_1^m)} \tag{3.62b}$$

Above relation is preserved under the renormalization transformation (3.54), in the sense that the constant A_m and B_m can be expressed as

$$A_m = u_r^{(m+1)}(r_{1/2}(t_0^{m+1}), t_0^{m+1})\nabla \cdot (u^{(m+1)}\nabla K * u^{(m+1)})|_{r=0}, \tag{3.63a}$$

$$B_m = \frac{1}{2}\nabla \cdot (u^{(m+1)}\nabla K * u^{(m+1)})|_{r=0} - \nabla \cdot (u^{(m+1)}\nabla K * u^{(m+1)})|_{r=r_{1/2}(t_0^{m+1})}, \tag{3.63b}$$

Because the renormalized function decays only algebraically even with a compactly supported initial data, the function $u^{(m)}$ is computed on a interval $r \in [0, L]$ and is chosen to be $u(L)(L/r)^{\alpha_m/\beta_m}$ for $r > L$.

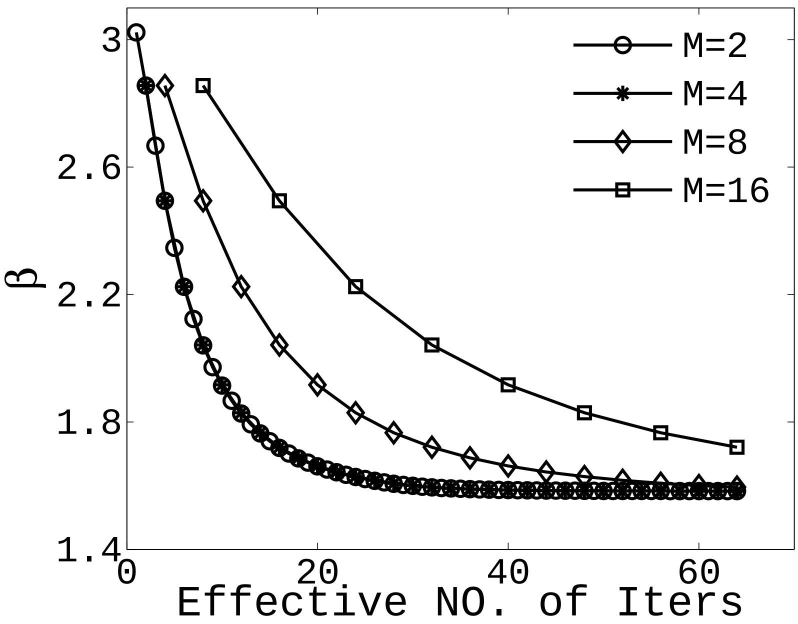

Figure 3.4: The convergence rate of the nuemerical renormalization method in dimension three for $\gamma = 1$. This rate is almost identitical for both $M = 2$ and $M = 4$ but can be slower when M becomes large.

When the larger M is, the longer it takes for one single RG iteration. The convergence rate of the exponent β for different M is shown in Figure 3.4 in dimension three for $\gamma = 1$. The number of iterations (called effective number of iterations in the figure) is rescaled such that the computational expense is roughly the same for the same number of iterations. Therefore, it is better to use a smaller M, say $M = 2$, rather than a larger one.

Since this numerical renormalization method is a fixed point iteration, it is not necessary convergent for any initial guess. Numerical experiments indicate that as long as we start with a function decaying fast enough, this iteration always converges. The convergence of the profile U is shown in Figure 3.5, in dimension three for $\gamma = 1$. The profile is already very close to the final profile after thirty iterations.

The anomalous exponent β computed using this numerical renormalization method is compared with that from direct simulation in Figure 3.12. The former concentrates the computation on the profile and the exponents with a fixed spatial domain while the latter have to resolve the solution on a large spatial domain and eventually cannot give a good fit at lower dimension when the kernel becomes singular. Therefore, the profile and the exponents can be computed with high accuracy without any formation of singularity. On the other hand, the direct simulation tells more details about the blowup dynamics, like various norms of the solution when approaching the blowup time.

For simulation in general dimensions, the auxiliary functions I_1, I_2 and I_3 are computed on 10^4 equally-spaced points on the interval $[0, 1]$. The number of spatial points is 4000 and the whole simulation takes a few days for one single dimension on a 3.0 GHz Intel Pentium IV cluster machine compiled with GNU GCC. For the special formulation in odd dimensions, the number of spatial points is as large as 2×10^4, and the simulation takes usually a few hours. Initially the grid points $\{r_j\}$ are placed such that $\ln(1 + r_j)$ is equally spaced on $[0, \ln(1 +$

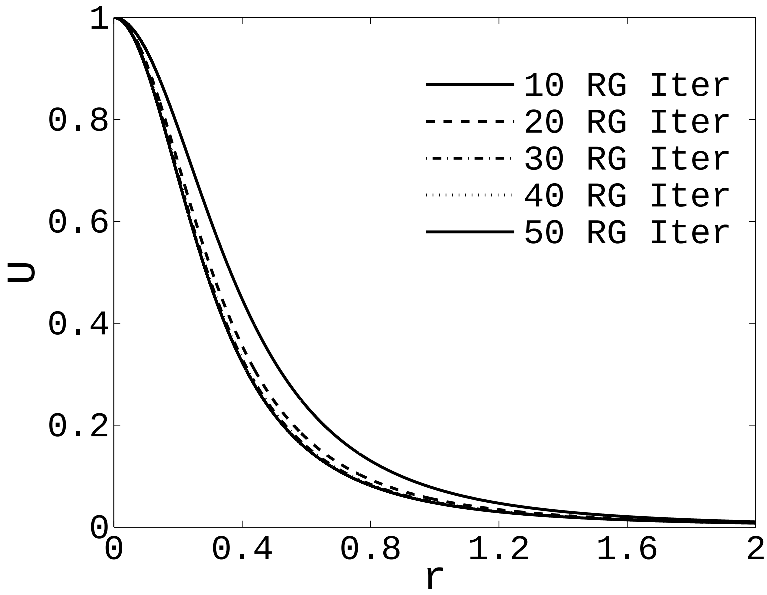

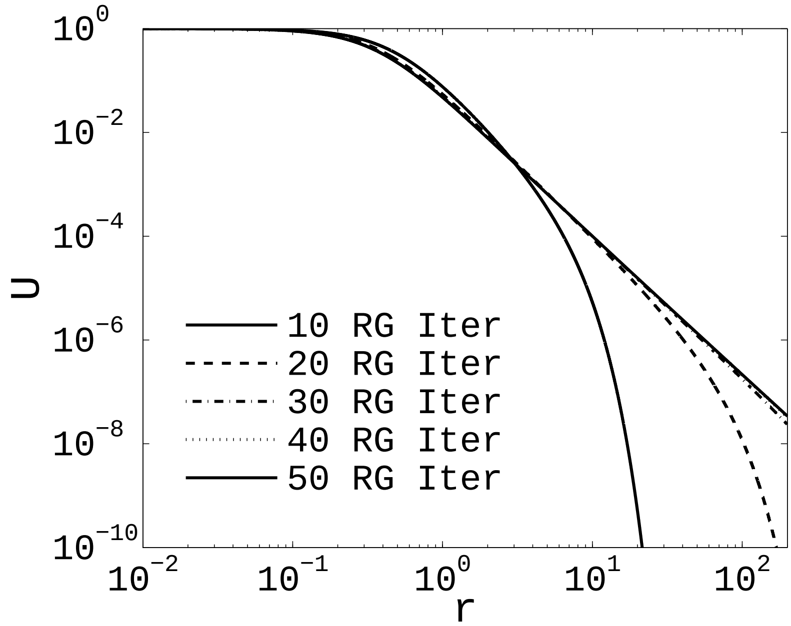

Figure 3.5: The convergence of the numerical renormalization method in dimension three for $\gamma = 1$. After thirty iteration, the profiles can not be distinguished from each other and are very close to the final profile.

$r_N)]$. The initial condition is chosen to be Gaussian, even though other smooth, compactly supported functions (not necessary to be radially decreasing) work well too and produce computationally identical similarity solutions. The special code for simulation in odd dimensions gives exponents α and β and other parameters consistent with code for general dimensions. The main difference is computational speed. We reiterate that we do not have to perform adaptive mesh refinement because the characteristics due a good job of following the similarity variables, although they are not identical.

3.2.5 Numerical Results

Here we use the same U to denote the blowup profile at different times and its final steady state, and later even the radially symmetric profile, when no confusion would arise. Moreover, it is easy to check that if $U(y)$ is a solution of above equation (3.7), so is

$$U_\lambda(y) = \lambda^{n+\gamma-2} U(\lambda y), \quad \lambda > 0 \tag{3.64}$$

and we have a family of profiles (see Section 3.1.2 for more discussion). Without loss of generality, any blowup profile shown below is normalized according to above scaling such that $U(0) = 1$.

The overall results show exact self-similar scaling in all dimensions studied. The normalized profiles ($U(0) = 1$) obtained from our simulations of the PDE, in different spatial dimensions, are shown in Figure 3.6-3.8. Near the origin, the profiles are ordered according to the dimension. Far away from the origin, due to different algebraic decay rate in different dimensions, these profiles are ordered. The algebraic tails (appearing as straight lines in the right log-log plot) will extend to infinity at the blowup time. The profiles for different γ are shown in Figure 3.9 for dimension three and in Figure 3.10 for dimension seven.

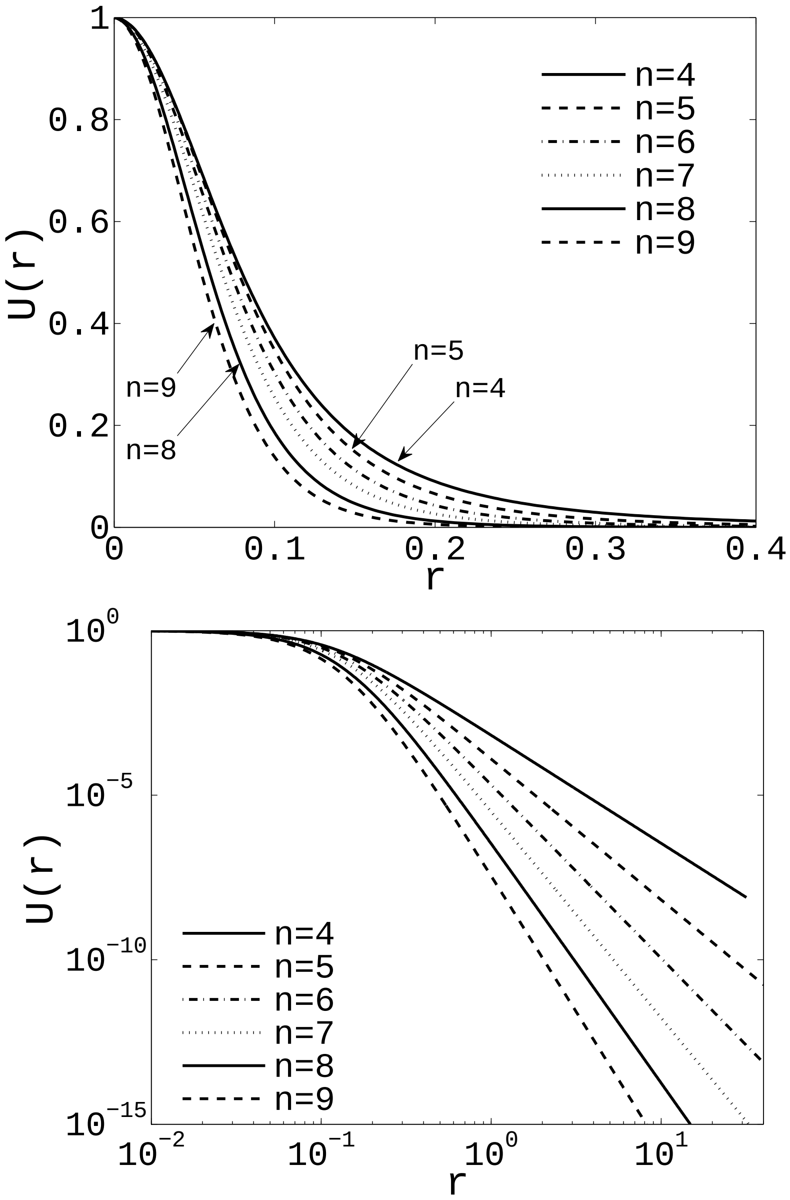

Figure 3.6: Similarity solution profiles show in the similarity variables U and $r = |y|$ as defined in (3.2-3.3), in different space dimensions for $\gamma = 0.4$, obtained by numerical integration of the PDE. All profiles are rescaled so that $U(0) = 1$ according to (3.64).

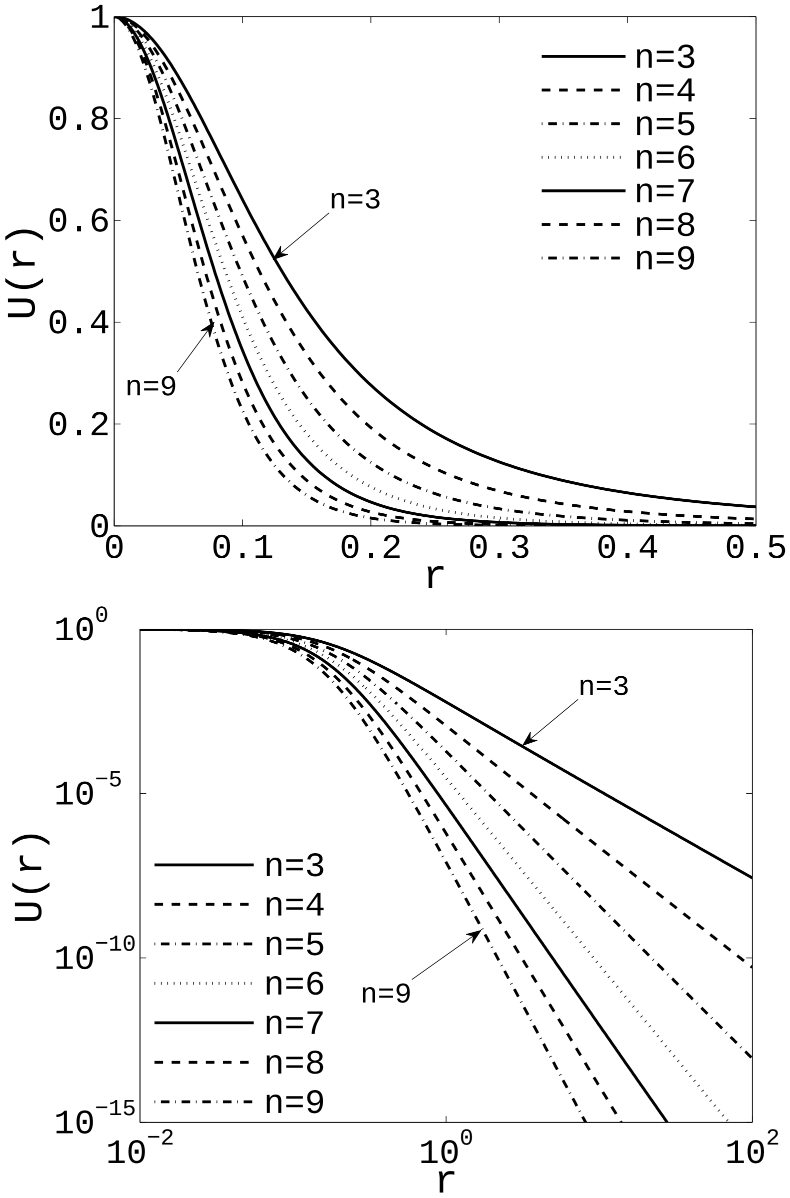

Figure 3.7: Similarity solution profiles show in the similarity variables U and $r = |y|$ as defined in (3.2-3.3), in different space dimensions for $\gamma = 1$, obtained by numerical integration of the PDE. All profiles are rescaled so that $U(0) = 1$ according to (3.64).

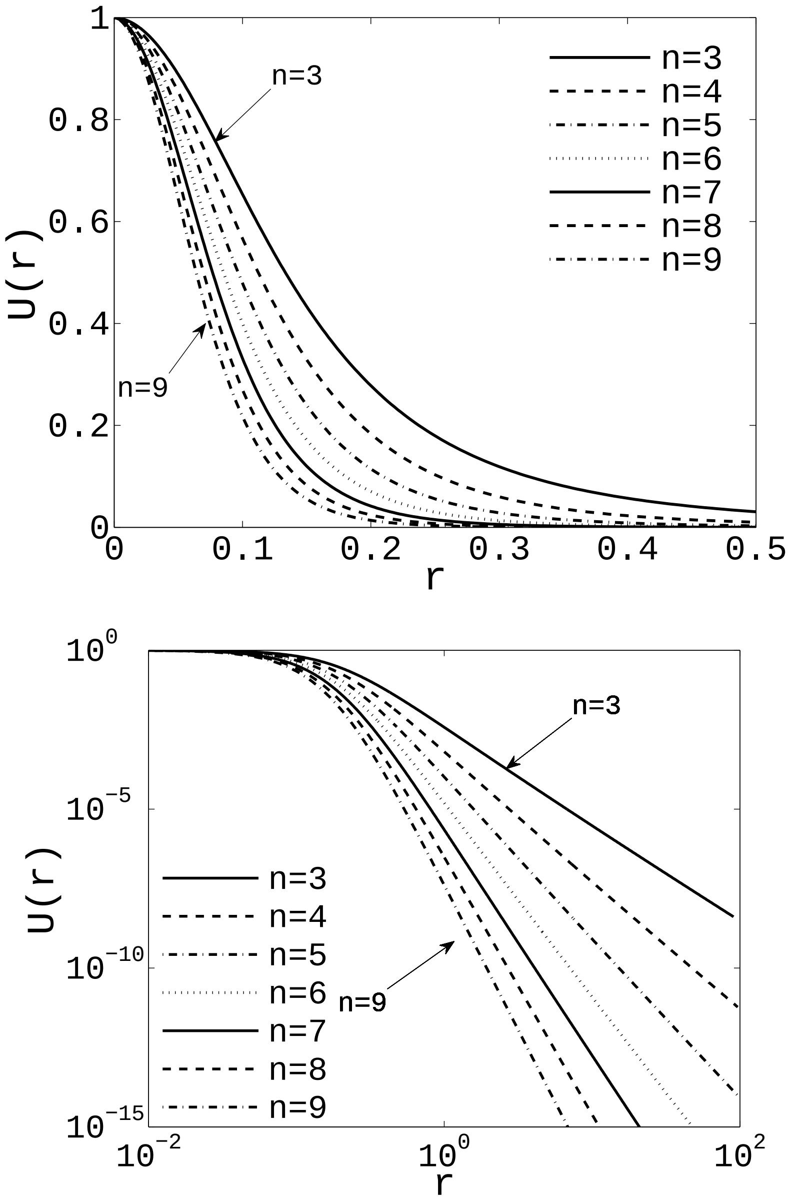

Figure 3.8: Similarity solution profiles show in the similarity variables U and $r = |y|$ as defined in (3.2-3.3), in different space dimensions for $\gamma = 1.6$, obtained by numerical integration of the PDE. All profiles are rescaled so that $U(0) = 1$ according to (3.64).

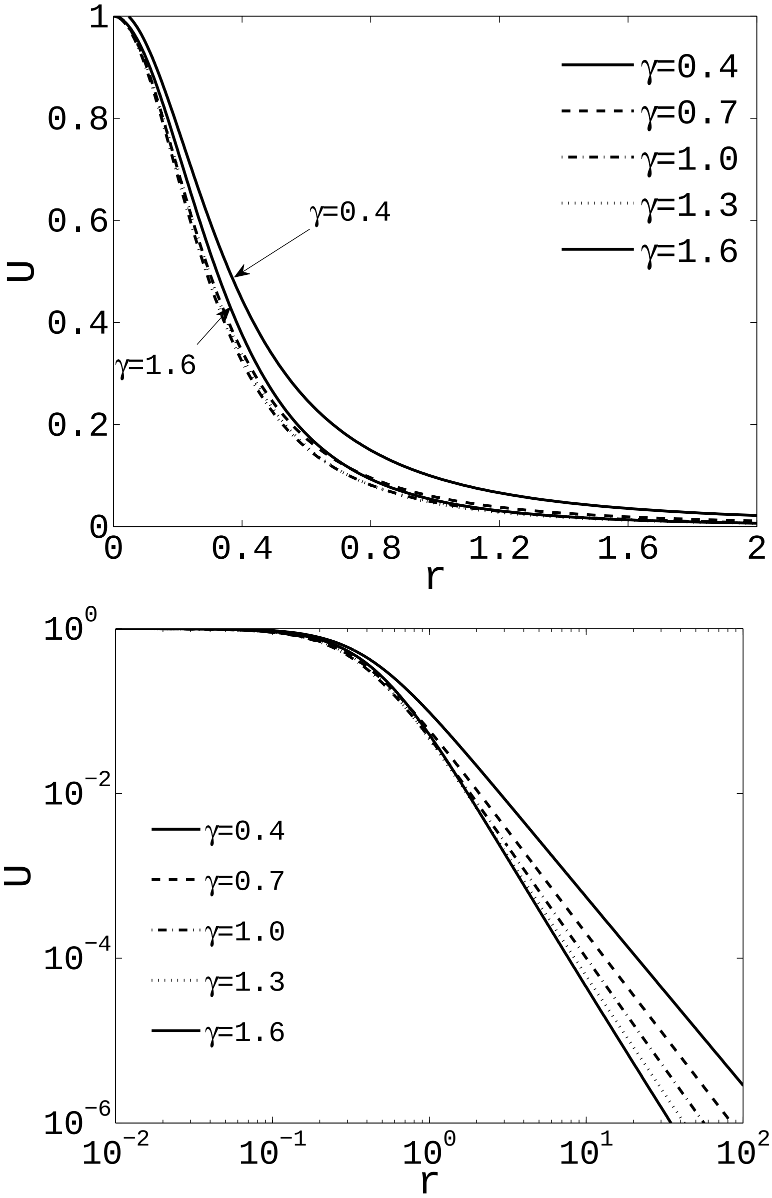

Figure 3.9: Similarity solution profiles show in the similarity variables U and $r = |y|$, in dimension three for different γ.

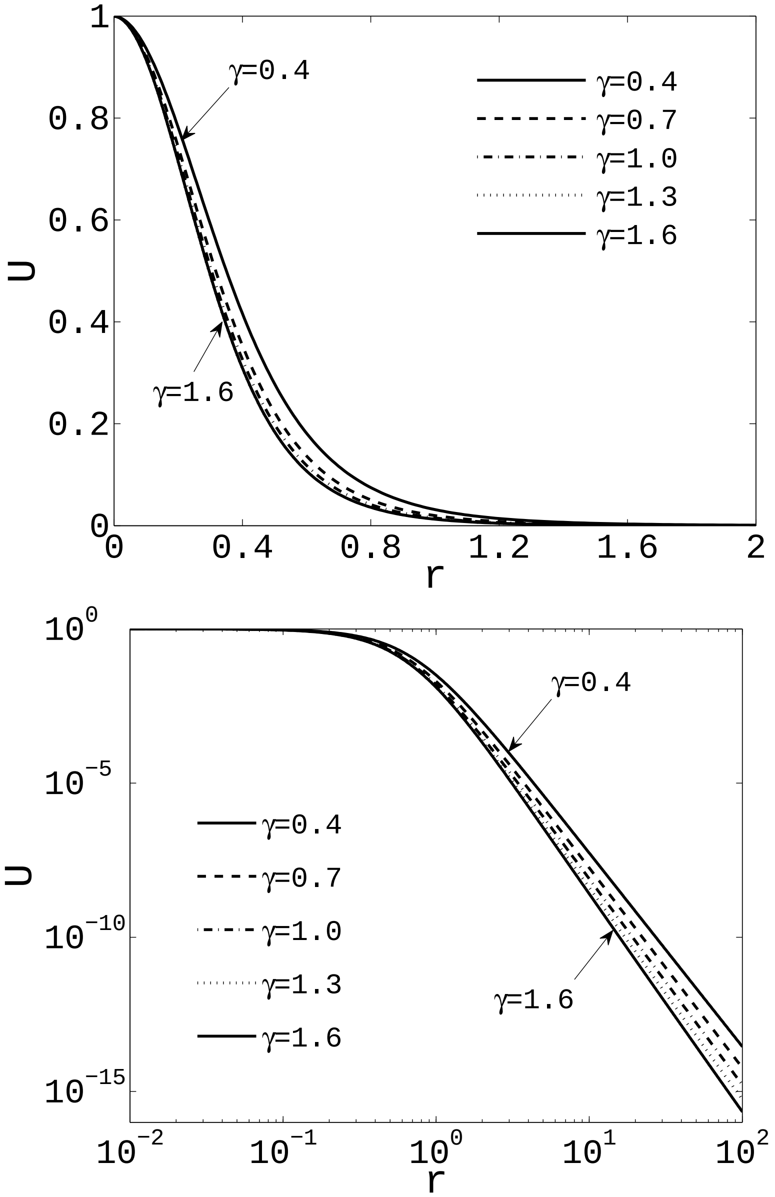

Figure 3.10: Similarity solution profiles show in the similarity variables U and $r = |y|$, in dimension seven for different γ.

Once we have the profiles, we can numerically check the validity of equation (3.7), which is shown in Figure 3.11 for dimension three. We observe that the part $\alpha U + \beta y \cdot \nabla U$ coming from the spatial-temporal scaling converges faster to a limit than the part associated with the kernel $\nabla \cdot (U \nabla K * U)$.

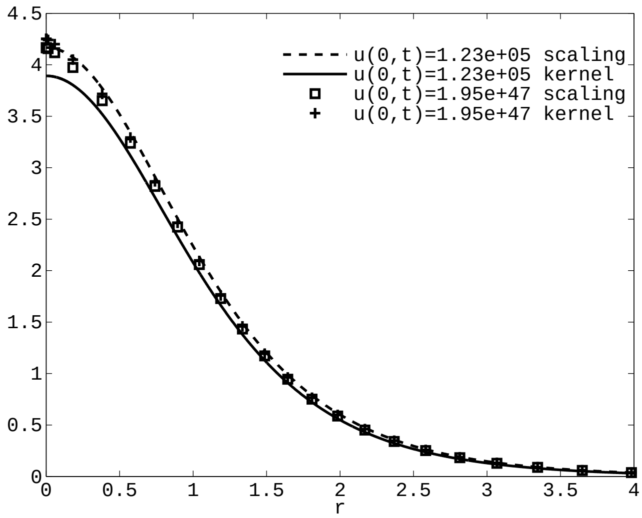

Figure 3.11: Comparison of the two contributions $\nabla \cdot (U \nabla K * U)$(kernel) and $\alpha U + \beta y \cdot \nabla U$(scaling) in equation (3.7) for different $u(0,t)$ in dimension three. The term $\alpha U + \beta y \cdot \nabla U$ (dash-dots) at smaller value of $u(0,t)$ is almost indistinguishable from both terms at larger value of $u(0,t)$.

The exponents α and β for $\gamma = 1$ are shown in Figure 3.12, by both post-processing of the data from the blowup dynamics and numerical renormalization group method. For radially symmetric solutions considered here, the computation can be extended to fractional dimension, giving more insight into the dependence of the parameters on the spatial dimension. In particular, the parameter β appears to increase with dimension.

The exponents β for different γ in different dimensions are shown in Figure 3.13. The dependence of β is much stronger on the exponent β than on the

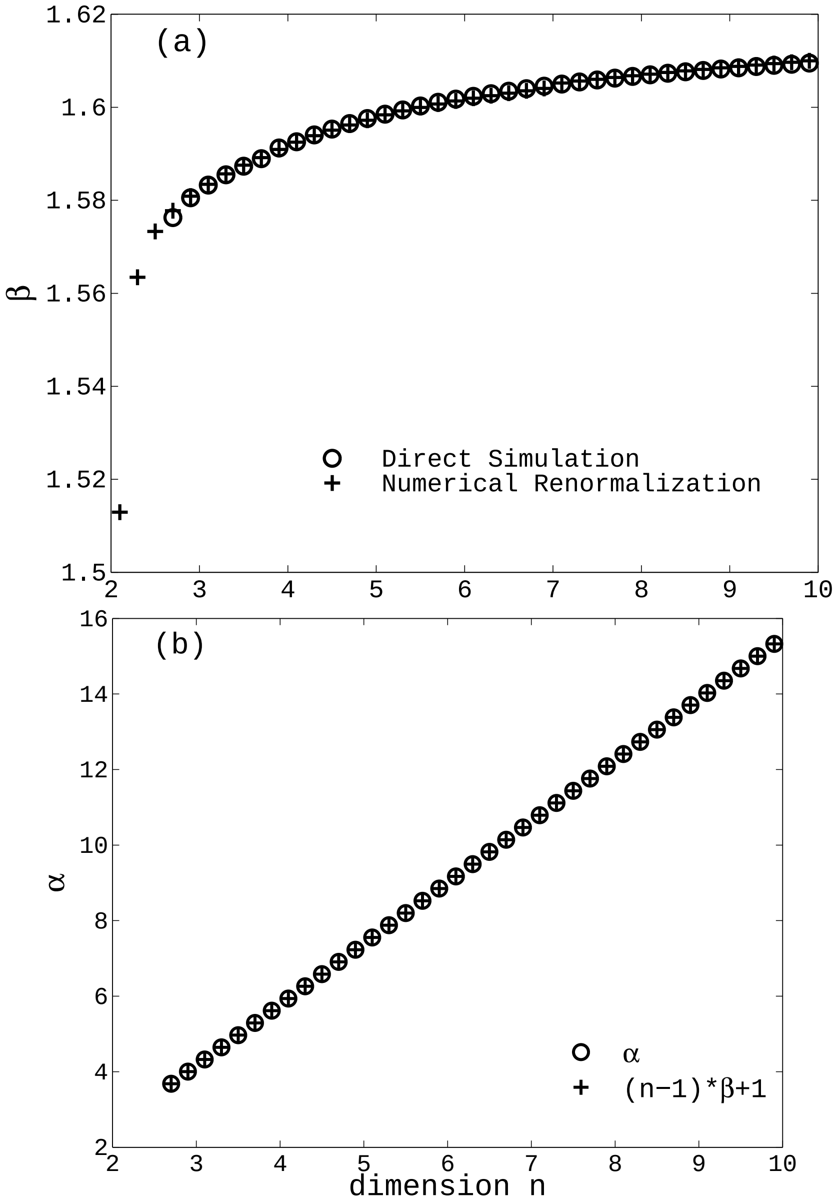

Figure 3.12: The exponents β and α characterizing the blowup in different spatial dimensions. The relation (3.5) is perfectly satisfied in the direct simulation while it is used exactly in the numerical renormalization.

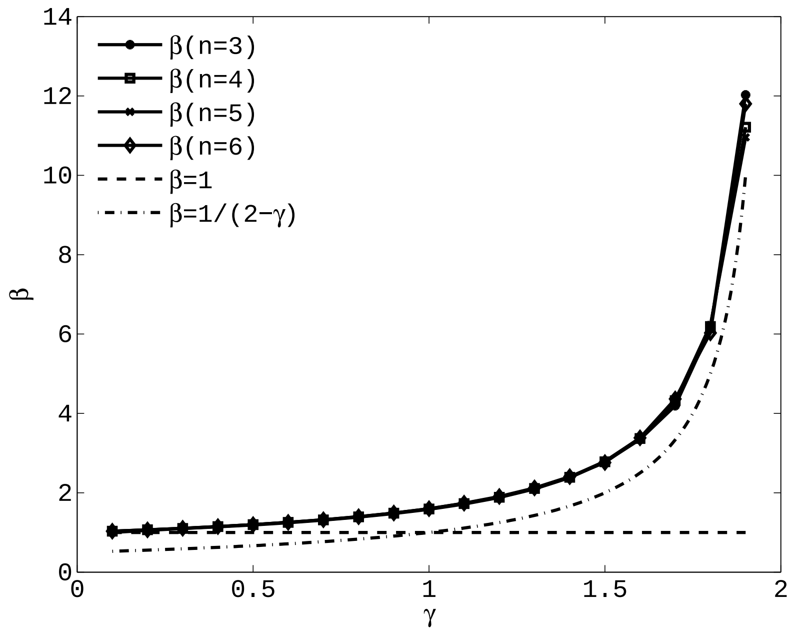

Figure 3.13: The anomalous exponent β in different dimension for different γ. This exponent has a weak dependence on the dimension n but a strong dependence on γ. We can clear see the asymptotic value of β to one when γ goes to zero.

dimension n; the increase of β for different dimensions is almost indistinguishable. From this figure, we can easily tell the asymptotic behaviors of β: when γ goes to zero, β goes to one; when γ goes to two, β goes to infinity. This observation motivates the perturbation expansion studied in later section.

We can have a closer look at the detailed blowup scenario in Figure 3.14 and 3.15 for the rescaled profile U and the original function u. Even though the results are presented only in dimension three and for $\gamma = 1$, it is generic in all dimensions for any γ. In Figure 3.14, the rescaled profiles $U(r, \tau)$ converges to the steady state quickly near the origin and the dynamics just adjusts the algebraic decay of the tails. In Figure 3.15, the original variable u is plotted at different

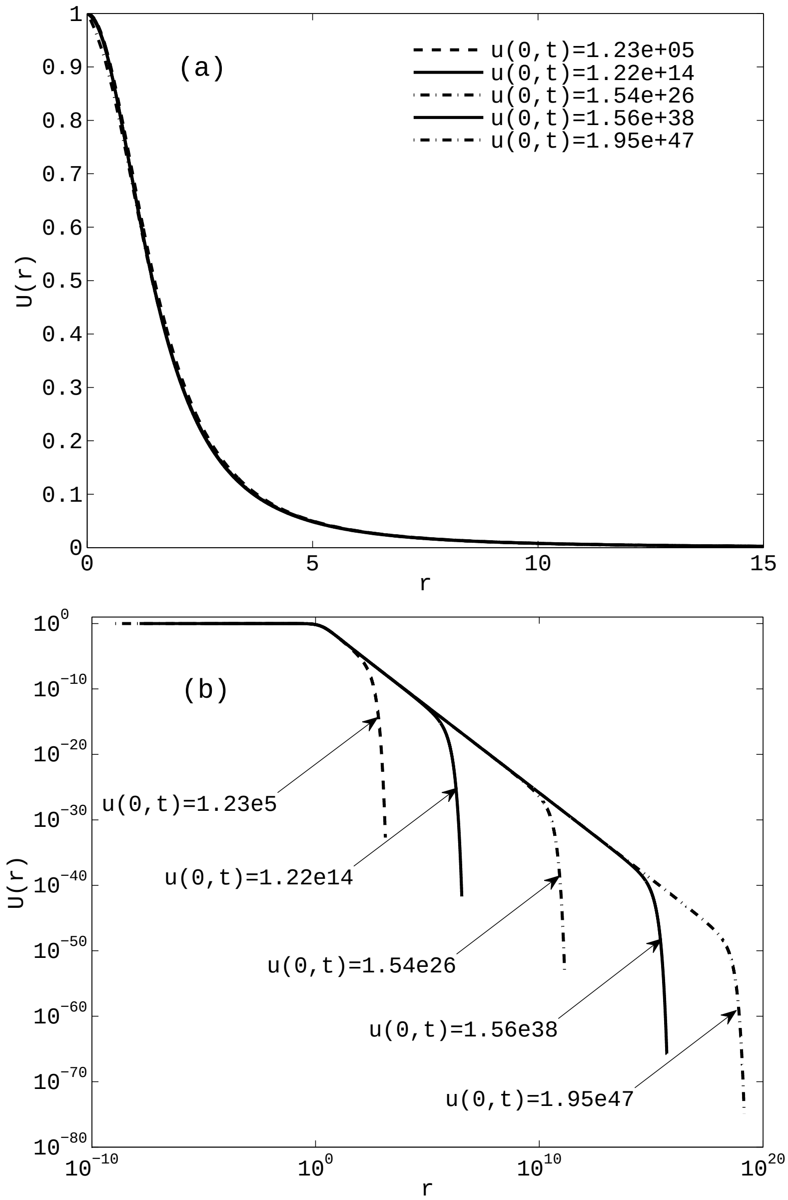

Figure 3.14: The convergence of the normalized profiles in dimension three. (a) Near the origin, all the profiles are indistinguishable. (b) Far away from the origin, the blowup dynamics adjusts the algebraic decay of the tail.

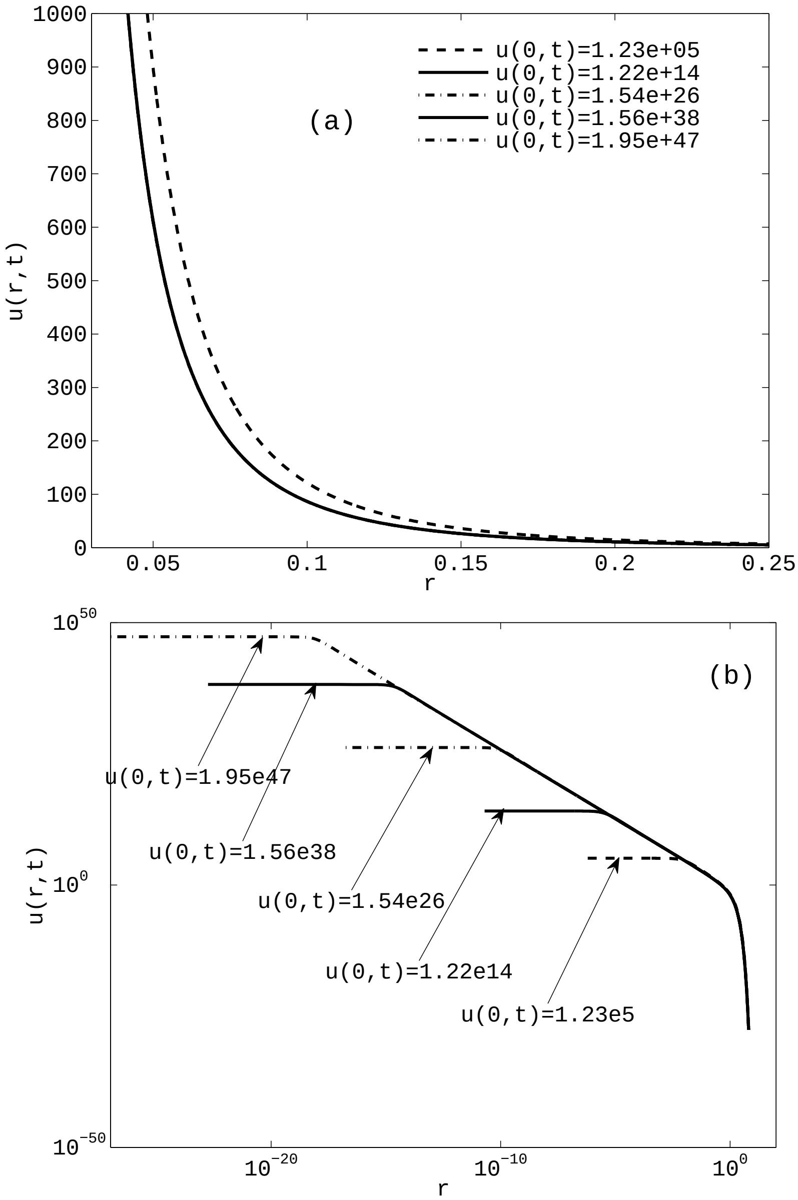

Figure 3.15: The convergence of the original function u in dimension three. (a) Away from the blowup point, the solution barely changes because the blowup happens in such a short time scale. (b) Close to the blowup point, the solution fills an envelope which becomes infinity at the origin.

stage during the blowup. Since the blowup takes place in such a short time, away form the core u barely changes. Near the blowup point, the solution fills an envelope when approaching the blowup time. Moreover, the algebraic decay of u and U are intimately related through the self-similar relation (3.3). In fact any fixed $|x| > 0$, $u(x,t) = (T-t)^{-\alpha}U(x(T-t)^{-\beta}, \tau)$ approaches a constant as $t \to T^-$. This gives the rate of algebraic decay for the steady profile U, $U(y) \sim |y|^{-\alpha/\beta} = |y|^{-(n-1+1/\beta)}$, making the part $\alpha U + \beta y \cdot \nabla U$ in the equation (3.7) vanish at leading order.

3.3 Exponents in Odd Dimension by Shooting Methods

3.3.1 Equivalent System and Shooting Methods

In radially symmetric coordinates, the steady equation (3.7) for the profile becomes

$$\nabla \cdot (U \nabla K * U) = \alpha U + \beta r \frac{\partial U}{\partial r}, \quad K(x) = |x| \tag{3.65}$$

with $\alpha = (n-1)\beta + 1 = 2N\beta + 1$.

We introduce additional variables $U_0(=U), U_1, \cdots, U_{N+1}$ such that

$$-\frac{1}{r^{2N}} \frac{d}{dr}\left(r^{2N} \frac{dU^{i+1}}{dr}\right) = U_i, \quad i = 0, 1, \cdots, N-1, \tag{3.66a}$$

$$\frac{1}{r^{2N}} \frac{d}{dr}\left(r^{2N} \frac{dU^{N+1}}{dr}\right) = k_N U_N, \tag{3.66b}$$

where k_N is a normalization constant defined to be

$$k_N = 2^N (2N+1) N! \frac{\pi^{\frac{2N+1}{2}}}{\Gamma(N+1+\frac{1}{2})} = \frac{2(4\pi)^N N!}{(2N-1)!!},$$

such that $U_{N+1} = K * U_0$. Under this transformation, the steay equation (3.65) can be written as

$$k_N U_N U_0 + \frac{dU_{N+1}}{dr}\frac{dU_0}{dr} = (2N\beta + 1)U_0 + \beta r \frac{dU_0}{dr}. \qquad (3.66c)$$

To put this system in a more convenient scaled form, we use the change of variables:

$$\zeta = \frac{r}{[(\beta - 1)/k_N]^{1/(2N)}}, \qquad (3.67a)$$

$$\begin{cases} U_i(r) = [(\beta - 1)/k_N]^{i/N} V_i(\zeta), \quad i = 0, 1, \cdots, N-1 \\ U_N(r) = \frac{2N+1}{k_N} + \frac{\beta-1}{k_N} V_N(\zeta), \\ U_{N+1}(r) = \frac{1}{2}\eta^2 + (\beta - 1)\left[\frac{\beta-1}{k_N}\right]^{1/N} V_{N+1}(\zeta), \end{cases} \qquad (3.67b)$$

yielding the final scaled (β and k_N independent) equations for the V's

$$V_N V_0 + \frac{dV_{N+1}}{d\zeta}\frac{dV_0}{d\zeta} = 2NV_0 + \zeta \frac{dV_0}{d\zeta}, \qquad (3.68a)$$

$$-\frac{1}{\zeta^{2N}}\frac{d}{d\zeta}\left(\zeta^{2N}\frac{dV_{i+1}}{d\zeta}\right) = V_i, \quad i = 0, 1, \cdots, N-1 \qquad (3.68b)$$

$$\frac{1}{\zeta^{2N}}\frac{d}{d\zeta}\left(\zeta^{2N}\frac{dV_{N+1}}{d\zeta}\right) = V_N. \qquad (3.68c)$$

The zero boundary conditions for U_i,$i = 1, 2, \cdots, N$ is now transformed to

$$V_0(\infty) = V_1(\infty) = \cdots = V_{N-1}(\infty) = 0, \quad V_N(\infty) = -\frac{2N+1}{\beta - 1}. \qquad (3.69)$$

With the right initial condition at $\zeta = 0$, we can recover the anomalous exponent β from the far field behavior of V_N.

This problem can be re-written as a system of first order equations in terms of variables

$$i = 0, 1, 2, \cdots, N, \qquad \begin{cases} z_{2i}(\zeta) = V_i(\zeta), \\ z_{2i+1}(\zeta) = V_i'(\zeta), \end{cases} \qquad (3.70)$$

or

$$\frac{dz_0}{d\zeta} = -\left(\frac{2N - z_{2N}}{\zeta - z_{2N+1}}\right) z_0, \tag{3.71a}$$

$$i = 1, 2, , \cdots, N, \qquad \begin{cases} \dfrac{dz_{2i-1}}{d\zeta} = -z_{2i-2} - \dfrac{2N}{\zeta} z_{2i-1}, \\ \dfrac{dz_{2i}}{d\zeta} = z_{2i-1}, \end{cases} \tag{3.71b}$$

$$\frac{dz_{2N+1}}{d\zeta} = z_{2N} - \frac{2N}{\zeta} z_{2N+1}. \tag{3.71c}$$

3.3.2 Shooting Method

Since the system (3.71) has a regular singular point at the origin, the system (3.71) is solved with any ODE solver starting at small $r = r_0 (> 0)$ with the initial condition at r_0 given by a convergent power series for z_i. For r near the original, we assume the following series expansion for z_0,

$$z_0(\zeta) = \sum_{k=0}^{\infty} u_{2k} \zeta^{2k}. \tag{3.72}$$

Only the even order terms survive due to the radial symmetry and all odds terms vanishes identically. Integrating the system (3.71) with the initial condition (or the shooting parameters), we have for i = 1,2,$\cdots$,N,

$$\begin{aligned} z_{2i-1}(\zeta) = (2N-1)!! \sum_{j=1}^{i-1} (-1)^j \frac{1}{2^{j-1}(j-1)!(2N+2j-1)!!} s_{i-j} \zeta^{2j-1} \\ + \frac{(-1)^i}{2^{i-1}} \sum_{k=0}^{\infty} \frac{k!(2k+2N-1)!!}{(k+i-1)!(2k+2N+2i-1)!!} u_{2k} \zeta^{2k+2i-1}, \end{aligned}$$

$$\begin{aligned} z_{2i}(\zeta) = (2N-1)!! \sum_{j=0}^{i-1} (-1)^j \frac{1}{2^j j!(2N+2j-1)!!} s_{i-j} \zeta^{2j} \\ + \frac{(-1)^i}{2^i} \sum_{k=0}^{\infty} \frac{k!(2k+2N-1)!!}{(k+i)!(2k+2N+2i-1)!!} u_{2k} \zeta^{2k+2i}, \end{aligned}$$

$$z_{2N+1}(\zeta) = k_N(2N-1)!!\sum_{j=0}^{N-1}(-1)^j\frac{1}{2^j j!(2N+2j+1)!!}s_{N-j}\zeta^{2j+1}$$
$$+\frac{(-1)^N k_N}{2^N}\sum_{k=0}^{\infty}\frac{k!(2k+2N-1)!!u_{2k}}{(k+N)!(2k+4N+1)!!}\zeta^{2k+2N+1}.$$

Substituting the expression z_0, z_{2N}, z_{2N+1} into the first equation in (3.71), we have

$$\begin{aligned}
& k_N\Bigg[(2N-1)!!\sum_{j=0}^{N-1}(-1)^j\frac{1}{2^j j!(2N+2j-1)!!}s_{N-j}\zeta^{2j} \\
& +\frac{(-1)^N}{2^N}\sum_{k=0}^{\infty}\frac{k!(2k+2N-1)!!u_{2k}}{(k+N)!(2k+4N-1)!!}r^{2k+2N}\Bigg]\sum_{k=0}^{\infty}u_{2k}\zeta^{2k} \\
+ \ & k_N\Bigg[(2N-1)!!\sum_{j=0}^{N-1}(-1)^j\frac{1}{2^j j!(2N+2j+1)!!}s_{N-j}\zeta^{2j} \\
& +\frac{(-1)^N}{2^N}\sum_{k=0}^{\infty}\frac{k!(2k+2N-1)!!u_{2k}}{(k+N)!(2k+4N+1)!!}\zeta^{2k+2N}\Bigg]\sum_{k=0}^{\infty}2ku_{2k}r^{2k} \\
= \ & \sum_{k=0}^{\infty}(2N+2k)u_{2k}\zeta^{2k}.
\end{aligned} \tag{3.73}$$

This gives the following recursive relations for the coefficients u_{2k},

$$u_{2j} = \frac{k_N(2N+1)!!(2N+2j+1)}{2j}\sum_{l=1}^{j}(-1)^l\frac{1}{2^l l!(2N+2l+1)!!}u_{2j-2l}s_{N-l}$$

for $j = 1, \cdots, N-1$ and

$$u_{2N+2k} = \frac{(-1)^N k_N(4N+2k+1)(2N+1)}{2^{N+1}(N+k)}\sum_{l=0}^{k}\frac{l!(2N+2l-1)!!}{(N+l)!(4N+2l+1)!!}u_{2l}u_{2k-2l}$$
$$+\frac{k_N(2N+1)!!(4N+2k+1)}{2(N+k)}\sum_{j=1}^{N-1}\frac{(-1)^j s_{N-j}}{2^j j!(2N+2j+1)!!}u_{2N+2k-2j}$$

for any interger $k \geq 0$.

The coefficients a_{2k} converges geometrically, and the correspoding power seiers has a finite radius of convergence (approximated 0.87 in dimension three). For small r_0, for a fixed shooting parameter ss, the initial condition $z_i(r_0)$ can be obtained with just a few terms in the expansion.

3.3.3 Numerical Results

For each shooting parameter $\mathbf{s} = (s_1, \cdots, s_{N-1}) = (z_2(0), \cdots, z_{2N-2}(0))$, we can find a direction $\delta\mathbf{s} = (\delta s_1, \delta s_2, \cdots, \delta s_{N-1})$ to make the far field condition $\tilde{\mathbf{z}}(L) = (z_2(L), z_4(L), \cdots, z_{2N-4}(L))$ as close to zero as possible for L large enough. Assuming a weak dependence on z_1, then the variation of $\tilde{\mathbf{z}}$ can be written as

$$\delta z_{2i}(L) = (2N-1)!! \sum_{j=0}^{i-1} \frac{(-1)^j}{2^j j!(2N+2j-1)!!} L^{2j} \delta s_{i-j}, \quad i = 1, 2, \cdots, N-1, \tag{3.74}$$

from which the variation $\delta\mathbf{s}$ can be solved in terms of δz_{2i}.

Once the variation $\delta\mathbf{s}$ is found, a fixed point iterative scheme can be constructed as

$$\mathbf{s}^{m+1} = \mathbf{s}^m - \omega\delta\mathbf{s}^m. \tag{3.75}$$

Here $\omega(< 1)$ is a positive relaxation parameter to stablize the iteration.

Because of the sensitive dependence of $u_{2N}(L)$ on the shooting parameters, the anomalous exponent β is recovered not by the last equatio in (3.69) but with the following equivalent but much more stable relation

$$\frac{2N\beta+1}{\beta-1} = z_{2N}(0) - z_{2N}(\infty) = \frac{1}{(N-1)!} \int_0^\infty \zeta^{2N} z_0(\zeta) d\zeta, \tag{3.76}$$

from successive integration of the system (3.71).

3.3.3.1 Dimension Three ($N = 1$)

Dimension three is special in the sense that there is no need for any shooting parameter. The anomalous exponent β is obtained from the solution of the sytem (3.71) via either (3.69) or (3.76), where the accuracy depends on the size of the interval $[0, L]$ we solve it. This is also compared with those by either direct similation of the blowup dynamic followed by data fitting or numerical renormalization group calculation performed in [HB10]. The computation time is at most a few seconds for the ODE system while at least a few hours for numerical RG.

	L	$\beta(n = 3)$	$\beta(n = 5)$	$\beta(n = 7)$	$\beta(n = 9)$
shooting method	10^2	1.580957	1.593860	1.574476	1.602537
shooting method	10^3	1.582976	1.598702	1.596328	1.607854
shooting method	10^4	1.583092	1.602900	N/A	N/A
numerical RG	400	1.582889	1.599152	1.604324	1.629743
Direct Computation	N/A	1.582226	1.598044	1.606732	1.623508

Table 3.1: Comparison of the computed anomalous exponents β from different methods in dimension three and higher.

3.3.3.2 Higher Dimension ($N \geq 2$)

Since the solution to the system (3.71) is not defined on the whole non-negative interval for certain shooting parameters when the denominator of the right hand side of the first equation in (3.71) changes sign and the assumption of weak dependence of z_{2i}s $i \geq 1$ on z_1 is not valid, the variation (3.74) is true only on part of the parameter space. This is is shown in Figure 3.3.3.1. The solution ceases to exist for $\mathbf{s}$ on the upper right region and the gradient field does not

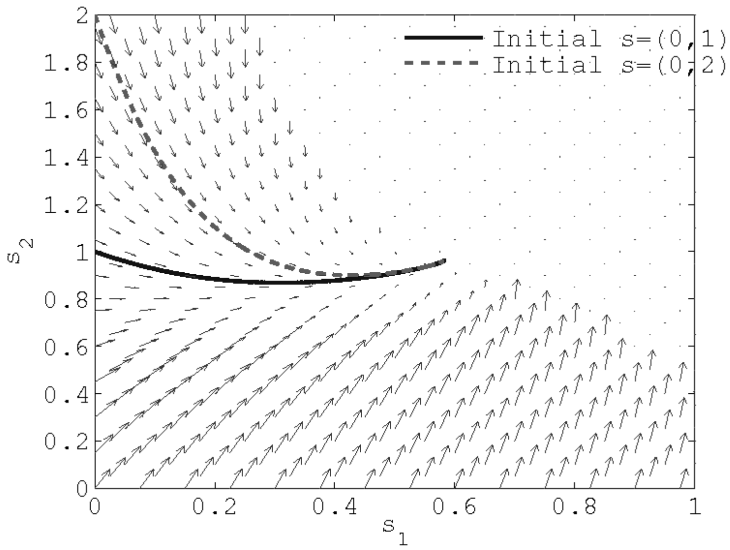

Figure 3.16: The gradient field and sample trajectories in dimension seven

lead us to the unique fixed point on the bottom region. However, once the initial guess $\mathbf{s}^0$ is in the basin of attraction, it alway converges to the unique fixed point. Numerical experiments indicate that the initial guess can be chosen as alternative large positive numbers and zeros from higer indices, i.e.

$$s^0_{N-1} = C,\ s^0_{N-2} = 0,\ s^0_{N-3} = C,\ \cdots \qquad \text{where } C \text{ is positive and large.} \quad (3.77)$$

The choice of $C = 2$ works for any test cases up to dimension fifteen. The numerical results are presented in Table (3.3.3.1), compared with those obtained from much slower computation of the full partial different equation.

3.4 The Case When $\epsilon = \gamma \to 0$

In general, the exponent β in the second-kind self-similar solution is governed by a nonlinear eigenvalue problem [AV95]. For the special case of $K(x) = |x|$ in odd dimension, the exponents are calculated by transforming the steady state equation (3.7) into a system of ODEs, followed a shooting method to match the boundary conditions of these two. Despite the difficulty of find it, the exponent β has a asymptotic limit when γ approaches zero and two. This is the subject of this and the next subsection.

When $\epsilon = \gamma \to 0$, we first rescale the solution U_ϵ to $W_\epsilon(x) = U_\epsilon(\epsilon^{1/(n+\epsilon-2)}x)$, since it is W_ϵ instead of U_ϵ that has a well-defined limit when $\epsilon \to 0$. The equation for W_ϵ is the same as U_ϵ except with the rescaled kernel $\tilde{K}_\epsilon(x) = |x|^\epsilon/\epsilon$, that is

$$\nabla \cdot (W_\epsilon \nabla \tilde{K}_\epsilon * W_\epsilon) = \alpha_\epsilon W_\epsilon + \beta_\epsilon r \frac{\partial W_\epsilon}{\partial r}. \tag{3.78}$$

The numerical results in Figure 3.13 suggests the following asymptotic expansion

$$\beta_\epsilon = 1 + C_1\epsilon + C_2\epsilon^2 + \cdots, \tag{3.79a}$$

$$\alpha_\epsilon = (n-2+\epsilon)\beta_\epsilon + 1 = n - 1 + ((n-2)C_1 + 1)\epsilon + \cdots \tag{3.79b}$$

and

$$W_\epsilon = W_0^{1+\epsilon V_1 + \epsilon^2 V_2 + \cdots} = W_0 + \epsilon V_1 W_0 \ln W_0 + \cdots. \tag{3.80}$$

The leading order equation in (3.78) is

$$\nabla \cdot (W_0 \nabla \ln|x| * W_0) = (n-1)W_0 + r\frac{\partial W_0}{\partial r}, \tag{3.81}$$

with the boundary conditions

$$W_0(0) = 1, \quad \frac{\partial W_0(0)}{\partial r} = 0, \quad W_0(r) \sim O(r^{1-n}) \quad \text{as } r \to \infty. \tag{3.82}$$

Define the linearized operator $\mathcal{L}_0$ for at W_0 as

$$\mathcal{L}_0(V) = \nabla \cdot (V \nabla \ln|x| * W_0) + \nabla \cdot (W_0 \nabla \ln|x| * V) - (n-1)V - x \cdot \nabla V. \tag{3.83}$$

Similarly by the invariance of the family of solutions $W_{0\lambda}(y) = \lambda^{n-2} W_0(\lambda y)$ we have

$$\mathcal{L}_0\left[(n-2)W_0 + y \cdot \nabla W_0\right] = 0. \tag{3.84}$$

The $O(\epsilon)$ in equation (3.78) is

$$\begin{aligned} \mathcal{L}_0(V_1 W_0 \ln W_0) &= ((n-2)C_1 + 1)W_0 + C_1 x \cdot \nabla W_0 - \nabla \cdot \left[W_0 \left(\frac{x}{|x|^2} \ln|x|\right) * W_0\right] \\ &= C_1 \mathcal{L}(W_0) - C_1 W_0 - \nabla \cdot \left[W_0 \left(\frac{x}{|x|^2} \ln|x|\right) * W_0\right]. \end{aligned} \tag{3.85}$$

Compared to (3.7) in general situations, there is no unknown parameters any more, even though it is still nonlinear and nonlocal.

Let $\mathcal{L}_0^*$ be the formal adjoint of $\mathcal{L}_0$, defined as

$$L_0^*(V) = -\nabla V \cdot \nabla \ln|x| * W_0 + \nabla_x \int \ln|x-y| W_0(y) \nabla V(y) dy - (n-1)V + \nabla \cdot (xV).$$

Since $\mathcal{L}_0$ has an one-dimensional null space, so does $\mathcal{L}_0^*$, spanned by some function W^*. The solvability condition for (3.85) is then obtained by mulitiplying both sides of it and integrating on the whole space, i.e.

$$\begin{aligned} 0 &= \int W^* \left(C_1 \mathcal{L}(W_0) - C_1 W_0 - \nabla \cdot \left[W_0 \left(\frac{x}{|x|^2} \ln|x|\right) * W_0\right]\right) dx \\ &= -C_1 \int W^* W_0 dx - \int W^* \nabla \cdot \left[W_0 \left(\frac{x}{|x|^2} \ln|x|\right) * W_0\right] dx \end{aligned} \tag{3.86}$$

or

$$C_1 = -\frac{1}{\int W^* W_0 dx} \int W^* \nabla \cdot \left[W_0 \left(\frac{x}{|x|^2} \ln|x|\right) * W_0\right] dx. \tag{3.87}$$

Compared to the equation of the profile in general cases, (3.81) does not have any unknown parameters. However, there is no easy way to solve this nonlinear, nonlocal integral-differential equation. By a smoothing method similar to the last section, we can solve it in even dimensions for the special kernel $\gamma = 1$. In figure 3.12, the first order correction and the numerically computed β are compared.

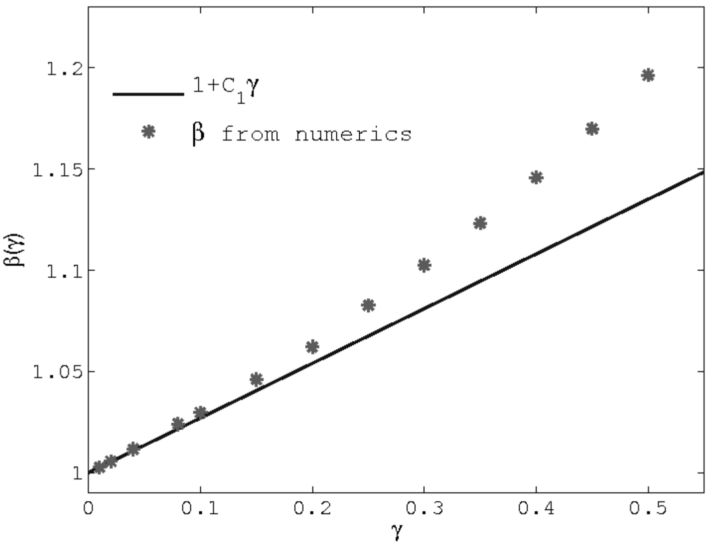

Figure 3.17: The comparison of the first order correction and the numerically computed β.

CHAPTER 4

Infinite Time Blowup: Convergence of the Delta-rings

When $\gamma \in (2, \infty)$, smooth solutions to the aggregation equation

$$u_t = \nabla \cdot (u \nabla K * u), \quad K(x) = |x|^\gamma \tag{4.1}$$

blows up only at infinite time according to the Osgood condition in [BCL09]. In this chapter, after applying a similarity transform, we show various properties of the transformed equation. For general initial condition, we show that the solution converges to some limit; for smooth, radially symmetric initial data, we show that the limit is a Dirac δ-ring and the detailed convergence to the this ring.

4.1 Similarity Transform

The intermediate asymptotics can be obtained with the introduction the following self-similar variables,

$$y = xt^\alpha, \quad \tau = \ln t, \quad U = t^{-\alpha} u \tag{4.2}$$

or $u(x,t) = t^\alpha U(xt^\beta, \tau)$. The new function U satisfies the equation

$$U_\tau = \nabla \cdot \left[U(\nabla \cdot K * U - \beta y) \right], \tag{4.3}$$

provided that

$$\alpha = \frac{n}{\gamma - 2}, \qquad \beta = \frac{1}{\gamma - 2}. \tag{4.4}$$

These exponents α and β are determined uniquely by the matching condition for the power of t in the equation and the conservation of the mass for U, while this is not true for the finite-time self-similar blowup solutions considered in the next section when $\gamma < 2$.

4.2 Convergence in the Similarity Variables

The long time behavior of the solution U is intimately related to the associated Lyapunov function, or the energy

$$E(U) = \frac{1}{2}\int_{\mathbb{R}^n}\int_{\mathbb{R}^n} K(x-y)U(x)U(y)dxdy - \frac{\beta}{2}\int_{\mathbb{R}^n} |x|^2 U(x)dx. \tag{4.5}$$

In fact, the solution U can be regarded as a gradient flow of this energy in the space of probability measure [Vil03, AGS08] of the form

$$\frac{\partial U}{\partial \tau} = -\mathrm{div}\left[U\left(\frac{\delta E}{\delta U}\right)\right] \tag{4.6}$$

and

$$\frac{d}{d\tau}E(U) = -\int_{\mathbb{R}^n} U(x)|\nabla K * U(x) - \beta x|^2 dx \leq 0. \tag{4.7}$$

To include the limiting solutions U, possibly Dirac-delta functions in the solution space, we consider the measure solution in the spaces

$$\mathcal{M} = \left\{\mu \text{ is a nonnegative Radon measure on } \mathbb{R}^n, \mu(\mathbb{R}^n) = M, \int_{\mathbb{R}^n} x d\mu = 0\right\}, \tag{4.8}$$

$$\mathcal{P}_\gamma(\mathbb{R}^n) = \left\{\mu \in \mathcal{M} : \int_{\mathbb{R}^n} |x|^\gamma d\mu < \infty\right\}. \tag{4.9}$$

By abuse of notation, we write $U(x)dx$ instead of $d\mu$ in the following. For any initial condition $U(\cdot, 0) \in \mathcal{P}_\gamma(\mathbb{R}^n)$, we can show that the $\gamma-$th order and thus second order moments are bounded uniformly at $\tau \to \infty$. In fact,

$$\begin{aligned}\int |x|^2 U(x)dx &= \frac{1}{2M}\int (|x|^2 + |y|^2 - 2x\cdot y)U(x)U(y)dxdy \\ &= \frac{1}{2M}\int\int |x-y|^2 U(x)U(y)dxdy. \end{aligned} \tag{4.10}$$

Using the Hölder's inequality

$$\int\int |x-y|^2 U(x)U(y)dxdy \le \left(\int\int |x-y|^\gamma U(x)U(y)dxdy\right)^{2/\gamma} M^{2-4/\gamma}, \tag{4.11}$$

we have

$$\begin{aligned} E(U) \ge \frac{1}{2}&\left(\int\int |x-y|^2 U(x)U(y)dxdy\right)^{\gamma/2} M^{2-\gamma} \\ &- \frac{\beta}{4M}\int\int |x-y|^2 U(x)U(y)dxdy. \end{aligned} \tag{4.12}$$

Since $\gamma > 2$, $E(U)$ is bounded below on $\mathcal{P}_\gamma(\mathbb{R}^n)$. Consequently, the boundness of the second order moments and the $\gamma-$th order moments implies the tightness of the sequence of solutions $U(\tau)$ in $\mathcal{P}_\gamma(\mathbb{R}^n)$. The weak compactness of the solutions $U(\tau)$ garantees the existence of limits U_∞ along some subsequence, proving the following theorem.

Theorem 4.2.1. *The solution $U(t)$ has a limit along some subsequence when t goes to infinity.*

Since $E(U)$ is bounded below, from the dissipation inequality (4.7), these limiting measures U_∞ satisfy the condition

$$\int U_\infty(y)|\nabla K * U_\infty - \beta y|^2 dy = 0. \tag{4.13}$$

In another word, U_∞ is concentrated on the set $\nabla K * U_\infty - \beta y$ vanishes. In the community of granular flow, for a given U_∞, the correspoding self-similar solution $u(x,t) = t^\alpha U_\infty(xt^\beta)$ is called homogeneous colling states [CV02], expected to

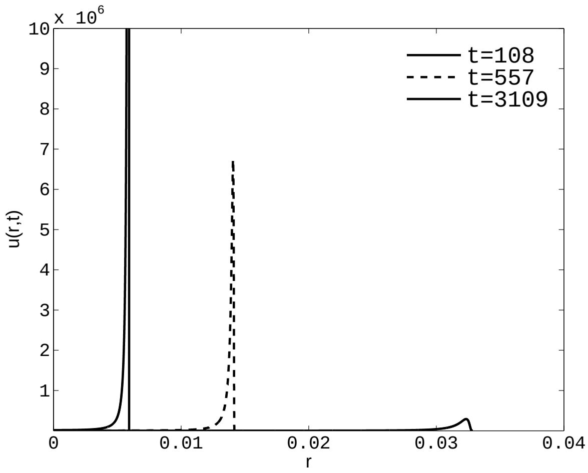

Figure 4.1: The solution u at different times

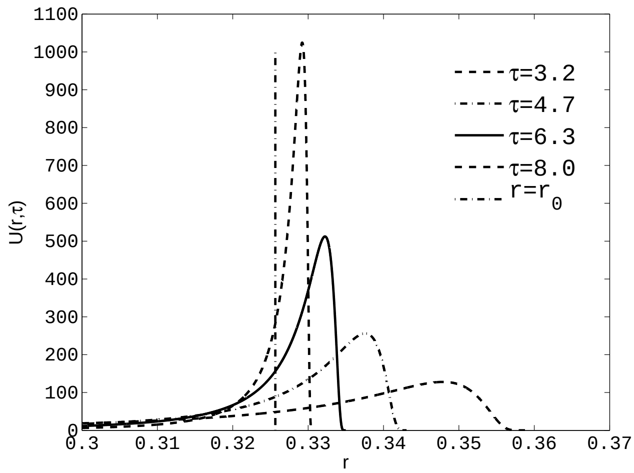

Figure 4.2: The solution U at different times

play the same role as the Maxwellian distribution for the Boltzmann equation in rarified gas dynamics.

However, because the energy $E(U)$ is not convex, the limits U_∞ above can be local minimizers or unstable equilibrium points. In general, the convergence of the solution to the limit U_∞ is so weak, there is no more information rather than the equality (4.13) characterizing it. This weak characterization can also be implied by the large family of solution. In dimension two, if L identical particles with total unit mass distributed uniformly on a circle of radius r, then the equilibrium condition (4.13) implies that

$$\beta r_L = \frac{\gamma}{L}\sum_{j=1}^{L-1}\left|1-e^{2\pi ji/L}\right|^{\gamma-2} r_L^{\gamma-1}(1-e^{2\pi ji/L}) \tag{4.14}$$

where $i=\sqrt{-1}$, the unit imaginary number. Then the equilibrium radius can be solved as

$$r_L = \left(\frac{L}{\gamma(\gamma-2)\sum_{j=1}^{L-1}\left(1-\cos\frac{2\pi j}{L}\right)\left(2-2\cos\frac{2\pi j}{L}\right)^{(\gamma-2)/2}}\right)^{1/(\gamma-2)}. \tag{4.15}$$

When the number of particles L goes to infinite, the radius r_L converges to the one for the δ-ring discussed in the next section, i.e.

$$r_\infty = \left(\gamma(\gamma-2)\int_0^1 (1-\cos 2\pi\theta)(2-2\cos\theta)^{(\gamma-2)/2}\right)^{-1/(\gamma-2)}. \tag{4.16}$$

Similarly it is easy to construct these saddle point solutions in higher dimension with particles distribution on the sphere with certain symmetry.

To get more qualitative properties, we consider only radially symmetric solutions in the rest of this section. Let

$$V(r) = \frac{d}{dr}K * U_\infty - \beta r, \tag{4.17}$$

since U_∞ is a nonnegative measure, $\frac{d^3}{dr^3}V(r) > 0$ on $[0,\infty)$ and $\frac{d^2}{dr^2}V(0) = 0$, $\frac{d}{dr}V(r)$ has at more one zero r_0 on $(0,\infty)$. In another word, by condition (4.13), U_∞ can only be be supported at the origin and r_0. If the fraction of mass concentrated at the origin is λ and the rest on the sphere of radius $r_{0,\lambda}$ is $1-\lambda$, or

$$U_{\infty,\lambda}(x) = \lambda M\delta(x) + \frac{(1-\lambda)M}{n\omega_n r_{0,\lambda}^{n-1}}\delta(|x| - r_{0,\lambda}) \tag{4.18}$$

then $r_{0,\lambda}$ con be solved from the equation $V'(r_{0,\lambda}) = 0$, giving the explicit value for the radius of mass concentrating sphere,

$$r_{0,\lambda} = \left(\frac{1}{\gamma M}\frac{\beta}{2\lambda + (1-\lambda)2^{\gamma-2}B(\frac{n+\gamma-2}{2},\frac{n-1}{2})/B(\frac{n-1}{2},\frac{n-1}{2})}\right)^{1/(\gamma-2)}. \tag{4.19}$$

where B is the Beta function.

We note that the limiting measure for $\lambda > 0$ is not stable: the amount of mass λM concentrated at the origin is exactly that from the initial condition; any perturbation of mass from the origin will concentrate to the sphere with positive radius instead of at the origin. In fact, the measure with $\lambda = 0$ corresponds to the global minimizer of the energy (4.5) while the one with $\lambda \neq 0$ is only a saddle point of the energy. For generic initial data without any concentration of mass at the origin, the solution U converges to the global minimizer $U_{\infty,0}$. Therefore, we consider the asymptotic behavior of U for this case and the generalization of it to the case $\lambda > 0$ requires only minor modification.

4.3 Asymptotic Convergence to the δ-Ring

For smooth initial data $U_0(y) = U(y,0)$ decaying fast enough, the solution to (4.3) stays smooth, though converging to a δ−ring. This brings the question of the intermediate asymptotics of U when τ is large. The key observation is that

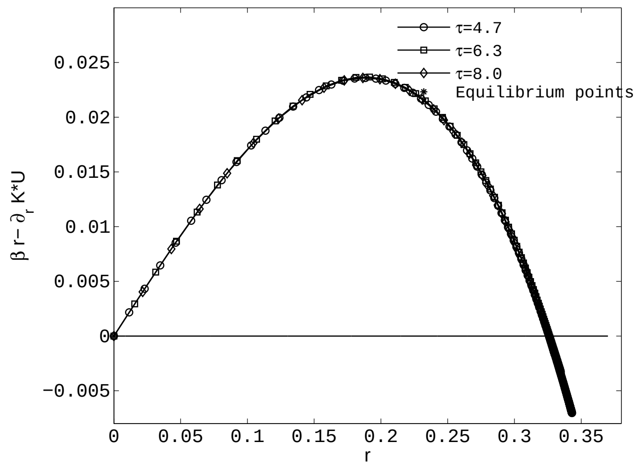

Figure 4.3: The characteristic velocity $dr/d\tau$

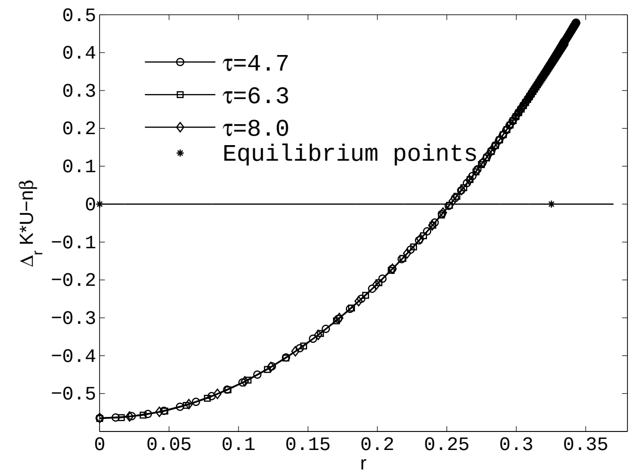

Figure 4.4: The rate of change of U

$K * U$ and its first and second derivatives change on a much slower scale than U itself, as shown in Figure 4.3 and 4.4, and the leading order asymptotics is governed by linear first order equation

$$U_\tau = \nabla \cdot [\nabla K * U_\infty - \beta y] \tag{4.20}$$

or the system of ODEs for the characteristic variables r and U

$$\begin{aligned} \frac{dr}{d\tau} &= \beta r - \frac{M\gamma}{\int_0^\pi \sin^{n-2}\theta d\theta} \int_0^\pi (r - r_0 \cos\theta)(r^2 + r_0^2 - 2rr_0\cos\theta)^{\gamma/2-1} \sin^{n-2}\theta d\theta, \\ \frac{dU}{d\tau} &= \frac{M\gamma(n+\gamma-2)U}{\int_0^\pi \sin^{n-2}\theta d\theta} \int_0^\pi (r^2 + r_0^2 - 2rr_0\cos\theta)^{\gamma/2-1} \sin^{n-2}\theta d\theta - n\beta. \end{aligned} \tag{4.21}$$

For $r < r_0$, above characteristic equations can be approximated as

$$\frac{dr}{d\tau} \approx A_0 r, \qquad \frac{dU}{d\tau} \approx (-B_0 + C_0 r^2)U \tag{4.22}$$

where

$$A_0 = \beta\left(1 - \frac{\gamma-1}{2^{\gamma-1}} \frac{B(\frac{n-1}{2}, \frac{n-1}{2})}{B(\frac{n+\gamma-1}{2}, \frac{n-1}{2})}\right), \tag{4.23}$$

$$B_0 = \beta\left(n - \frac{n+\gamma-2}{2^{\gamma-2}} \frac{B(\frac{n-1}{2}, \frac{n-1}{2})}{B(\frac{n+\gamma-1}{2}, \frac{n-1}{2})} -\right), \tag{4.24}$$

$$C_0 = \beta\left(1 - \frac{\gamma-2}{2^{\gamma-2}} \frac{B(\frac{n-1}{2}, \frac{n-1}{2})}{B(\frac{n+\gamma-1}{2}, \frac{n-1}{2})} -\right), \tag{4.25}$$

$$\tag{4.26}$$

leading to asymptotics form of the solution

$$U(r,\tau) \sim U_0(s) e^{-B_0\tau + \frac{C_0}{3}r^2} \sim e^{-B_0\tau + \frac{C_0}{3}r^2} \tag{4.27}$$

This implies that the decay of the solution at the origin is $e^{-B_0\tau}$, comfirmed numerically in Figure 4.6 and the increase of the solution near the origin is

$$U(r,\tau) \sim U(0,\tau) e^{C_0 r^2/3},$$

comfirmed numerically in Figure 4.7.

For r exponentially close to r_0, the characteristic equations can be approximated as

$$\frac{dr}{d\tau} \approx -A_1(r - r_0), \qquad \frac{dU}{d\tau} \approx B_1 - C_1(r - r_0) \tag{4.28}$$

leading to the asymptotic form

$$U(r,\tau) \sim e^{B_1\tau + C_1 e^{A_1\tau}(r-r_0)/A_1}. \tag{4.29}$$

In general, we can only get the order of magnitude as above (4.27) and (4.29), while the prefactor depends on the initial condition U_0 and the transit behavior when $K * U$ is replaced by $K * U_\infty$.

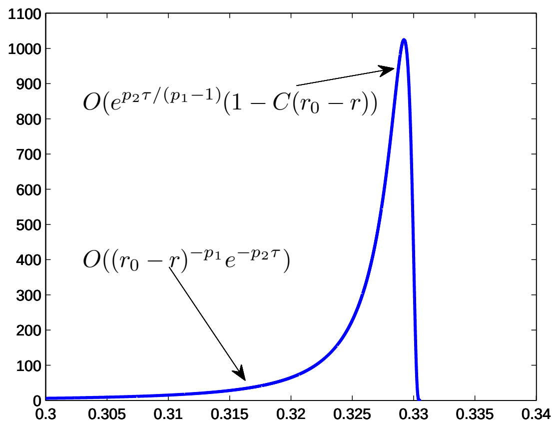

Figure 4.5: The asymptotic form approaching the ring profile

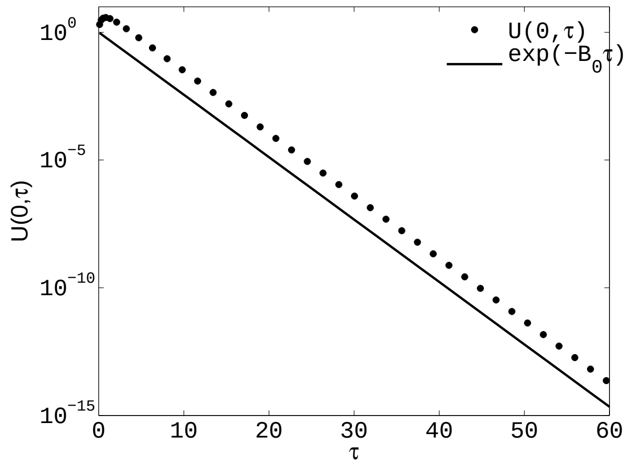

Figure 4.6: Comparison of the asymptotic ring profile with that from eqaution (4.22).

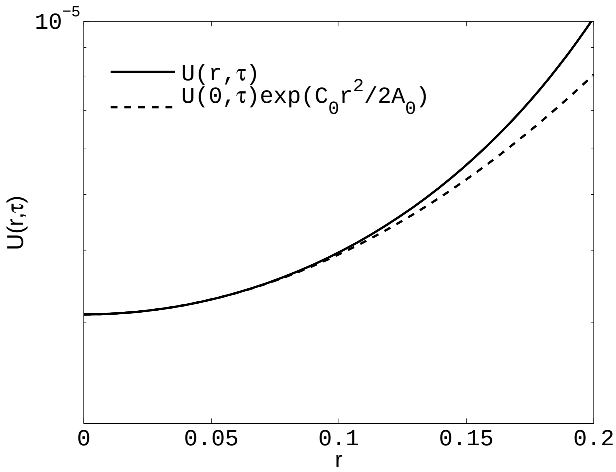

Figure 4.7: The asymptotic decay of $U(0, \tau)$: Numerical simulation and the asymptotics form

CHAPTER 5

Conclusion and Future Works

This thesis focuses on the radially symmetric solutions with smooth initial data for the aggregation equation in its simplest form and with the special homogeneous power-law kernel $K(x) = |x|^\gamma$. When $\gamma \in (0, 2)$, the self-similar solutions are of the second kind and we have to rely on high resolution numerics to find the blowup profiles and the anomalous exponents. When $\gamma \in (2, \infty)$, the asymptotic behaviors of the solutions can be obtained by a similarity transform. All these results can be extended in various general settings.

Even though it is unlikely to find exact self-similar solutions and other quantitative information for the non-radially symmetry problem, it is interesting to know the stability of the solutions under perturbation. When $\gamma \in (2, \infty)$, because of the existence of the Lyapunov function, all smooth perturbations do not change the final limit. In contrast, when $\gamma \in (0, 2)$, there is not much known and numerical renormalization study, similar to those done for porous medium equation in [BAA00] can be prolific.

In this thesis, we consider only the blowup of solutions with smooth initial data. The solutions cease to exist as smooth functions or Sobolev functions in $L^p(\mathbb{R}^n)$. However, these solutions can be continued in more general sense, as measured-valued solutions [CDF10]. Right after the blowup time, the solutions can be written as the combination of a smooth part and a singular part. It is interesting to know the interaction of these two parts.

The aggregation equation we considered here is in its simplest form. There are many variants of it, notably with diffusion, either degenerate or diffusion. Unusually, because of the presence of diffusion effects, the solutions are less likely to blowup and possibly converges to smooth steady solutions. Because of the extra length scale associated with diffusion, the self-similar solutions, if they exists, are more likely to be of the first kind. It is also interesting to know the detailed behavior of the transition of these similarity solutions of the first kind to those of the second kind, when the diffusion vanishes.

References

[AA95] S. B. Angenent and D. G. Aronson. "The focusing problem for the radially symmetric porous medium equation." *Comm. Partial Differential Equations.*, **20**(7-8):1217–1240, 1995.

[AG93] D. G. Aronson and J. Graveleau. "A self-similar solution to the focusing problem for the porous medium equation." *European J. Appl. Math.*, **4**(1):65–81, 1993.

[AGS08] Luigi Ambrosio, Nicola Gigli, and Giuseppe Savaré. *Gradient flows in metric spaces and in the space of probability measures.* Lectures in Mathematics ETH Zürich. Birkhäuser Verlag, Basel, second edition, 2008.

[Ali95] Serge Alinhac. *Blowup for nonlinear hyperbolic equations.* Progress in Nonlinear Differential Equations and their Applications, 17. Birkhäuser Boston Inc., Boston, MA, 1995.

[AV95] D. G. Aronson and J. L. Vázquez. "Anomalous exponents in nonlinear diffusion." *J. Nonlinear Sci.*, **5**(1):29–56, 1995.

[BAA00] S. I. Betelú, D. G. Aronson, and S. B. Angenent. "Renormalization study of two-dimensional convergent solutions of the porous medium equation." *Phys. D*, **138**(3-4):344–359, 2000.

[Bar96] G. I. Barenblatt. *Scaling, self-similarity, and intermediate asymptotics*, volume 14 of *Cambridge Texts in Applied Mathematics.* Cambridge University Press, Cambridge, 1996.

[BB10] A. L. Bertozzi and J. Brandman. "Finite-time blow-up of L^∞-weak solutions of an aggregation equation." *Commun. Math. Sci.*, **8**(1):45–65, 2010.

[BBW98] A. J. Bernoff, A. L. Bertozzi, and T. P. Witelski. "Axisymmetric surface diffusion: dynamics and stability of self-similar pinchoff." *J. Statist. Phys.*, **93**(3-4):725–776, 1998.

[BCK99] M. P Brenner, P. Constantin, L P. Kadanoff, A. Schenkel, and S. C.Venkataramani. "Diffusion, attraction and collapse." *Nonlinearity*, **12**(4):1071–1098, 1999.

[BCL09] A. L. Bertozzi, J. A. Carrillo, and T. Laurent. "Blow-up in multidimensional aggregation equations with mildly singular interaction kernels." *Nonlinearity*, **22**(3):683–710, 2009.

[BCM00] S. Boi, V. Capasso, and D. Morale. "Modeling the aggregative behavior of ants of the species Polyergus rufescens." *Nonlinear Analysis: Real World Applications*, **1**(1):176, 2000.

[BCR05] C. J. Budd, R. Carretero-González, and R. D. Russell. "Precise computations of chemotactic collapse using moving mesh methods." *J. Comput. Phys.*, **202**(2):463–487, 2005.

[BG98] C. J. Budd and V. A. Galaktionov. "Stability and spectra of blow-up in problems with quasi-linear gradient diffusivity." *R. Soc. Lond. Proc. Ser. A Math. Phys. Eng. Sci.*, **454**(1977):2371–2407, 1998.

[BGW04] C. J. Budd, V. A. Galaktionov, and J. F. Williams. "Self-similar blow-up in higher-order semilinear parabolic equations." *SIAM J. Appl. Math.*, **64**(5):1775–1809 (electronic), 2004.

[BHR96] Chris J. Budd, Weizhang Huang, and Robert D. Russell. "Moving mesh methods for problems with blow-up." *SIAM J. Sci. Comput.*, **17**(2):305–327, 1996.

[BKM84] J. T. Beale, T. Kato, and A. Majda. "Remarks on the breakdown of smooth solutions for the 3-D Euler equations." *Comm. Math. Phys.*, **94**(1):61–66, 1984.

[BL07] A. L. Bertozzi and T. Laurent. "Finite-time blow-up of solutions of an aggregation equation in $\mathbb{R}^n$." *Comm. Math. Phys.*, **274**(3):717–735, 2007.

[BL09] A. L. Bertozzi and T. Laurent. "The behavior of solutions of multidimensional aggregation equations with mildly singular interaction kernels." *Chinese Annals of Mathematics, Series B*, **30**(5):463–482, 2009.

[BRB10] Jacob Bedrossian, Nancy Rodriguez, and Andrea Bertozzi. "Local and global well-posedness for aggregation equations and Patlak-Keller-Segel models with degenerate diffusion.", 2010. submitted.

[BS69] G. I. Barenblatt and G. I. Sivashinskii. "Self-similar solutions of the second kind in nonlinear filtration." *J. Appl. Math. Mech.*, **33**:836–845, 1969.

[BS10] Andrea L. Bertozzi and Dejan Slepcev. "Existence and uniqueness of solutions to an aggregation equation with degenerate diffusion.", 2010. To appeear in Comm. Pure. Appl. Anal.

[Bur74] J.M. Burgers. *The nonlinear diffusion equation: asymptotic solutions and statistical problems*. Springer, 1974.

[BV06] M. Bodnar and J. J. L. Velazquez. “An integro-differential equation arising as a limit of individual cell-based models.” *J. Differential Equations*, **222**(2):341–380, 2006.

[BW98] M. P. Brenner and T. P. Witelski. “On spherically symmetric gravitational collapse.” *J. Statist. Phys.*, **93**(3-4):863–899, 1998.

[CDF10] J. A. Carrillo, M. DiFrancesco, A. Figalli, T. Laurent, and D. Slepcev. “Global-in-time weak measure solutions, finite-time aggregation and confinement for nonlocal interaction equations.”, 2010. To appear in Duke Mathematical Journal.

[CG95] L.Y. Chen and N. Goldenfeld. “Numerical renormalization-group calculations for similarity solutions and traveling waves.” *Physical Review E*, **51**(6):5577–5581, 1995.

[CGT64] R. Y. Chiao, E. Garmire, and C. H. Townes. “Self-trapping of optical beams.” *Phys. Rev. Lett.*, **13**(15):479–482, Oct 1964.

[CHD07] Y.L. Chuang, Y.R. Huang, M.R. D’Orsogna, and A.L. Bertozzi. “Multi-vehicle flocking: scalability of cooperative control algorithms using pairwise potentials.” In *2007 IEEE International Conference on Robotics and Automation*, pp. 2292–2299, 2007.

[CMT94] Peter Constantin, Andrew J. Majda, and Esteban Tabak. “Formation of strong fronts in the 2-D quasigeostrophic thermal active scalar.” *Nonlinearity*, **7**(6):1495–1533, 1994.

[Con94] Peter Constantin. “Geometric statistics in turbulence.” *SIAM Rev.*, **36**(1):73–98, 1994.

[CV02] E. Caglioti and C. Villani. “Homogeneous cooling states are not always good approximations to granular flows.” *Arch. Ration. Mech. Anal.*, **163**(4):329–343, 2002.

[CW96] Julian D. Colea and Barbara A. Wagnera. “On self-similar solutions of Barenblatt’s nonlinear filtration equation.” *European J. Appl. Math.*, **7**:151–167, 1996.

[DH] P. Debye and E Hückle. “The theory of electrolytes. I. Lowering of freezing point and related phenomena.” *Physikalische Zeitschrift*, **24**:185–206.

[Dol85] J. W. Dold. "Analysis of the early stage of thermal runaway." *The Quarterly Journal of Mechanics and Applied Mathematics*, **38**(3):361–387, 1985.

[Don10] Hongjie Dong. "The aggregation equation with power-law kernels: ill-posedness, mass concentration and similarity solutions.", 2010. submitted.

[DZ03] Q. Du and P. Zhang. "Existence of weak solutions to some vortex density models." *SIAM Journal on Mathematical Analysis*, **34**(6):1279–1299, 2003.

[EF09] Jens Eggers and Marco A. Fontelos. "The role of self-similarity in singularities of partial differential equations." *Nonlinearity*, **22**(1):R1–R44, 2009.

[Eva10] Lawrence C. Evans. *Partial differential equations*, volume 19 of *Graduate Studies in Mathematics*. American Mathematical Society, Providence, RI, second edition, 2010.

[FGW05] Gadi Fibich, Nir Gavish, and Xiao-Ping Wang. "New singular solutions of the nonlinear Schrödinger equation." *Phys. D*, **211**(3-4):193–220, 2005.

[Fis37] RA Fisher. "The wave of advance of advantageous genes." *Ann. Eugenics*, **7**(353):269, 1937.

[FK92] Stathis Filippas and Robert V. Kohn. "Refined asymptotics for the blowup of $u_t - \Delta u = u^p$." *Comm. Pure Appl. Math.*, **45**(7):821–869, 1992.

[Fuj66] H. Fujita. "On the blowing up of solutions of the Cauchy problem for $u_t = \Delta u + u^{1+\alpha}$." *J. Fac. Sci. Univ. Tokyo Sect. I*, **13**:109–124, 1966.

[GK85] Yoshikazu Giga and Robert V. Kohn. "Asymptotically self-similar blow-up of semilinear heat equations." *Comm. Pure Appl. Math.*, **38**(3):297–319, 1985.

[Gla77] R. T. Glassey. "On the blowing up of solutions to the Cauchy problem for nonlinear Schrödinger equations." *Journal of Mathematical Physics*, **18**(9):1794–1797, 1977.

[GMO90] Nigel Goldenfeld, Olivier Martin, Y. Oono, and Fong Liu. "Anomalous dimensions and the renormalization group in a nonlinear diffusion process." *Phys. Rev. Lett.*, **64**(12):1361–1364, Mar 1990.

[GP02] V. Gazi and K.M. Passino. "Stability analysis of swarms." In *American Control Conference, 2002. Proceedings of the 2002*, pp. 1813–1818, 2002.

[HB10] Yanghong Huang and Andrea L. Bertozzi. "Self-similar blowup solutions to an aggregation equation in R^n." *SIAM J. Appl. Math.*, **70**(7):2582–2603, 2010.

[HMR08] W. Huang, J. Ma, and R. D. Russell. "A study of moving mesh PDE methods for numerical simulation of blowup in reaction diffusion equations." *J. Comput. Phys.*, **227**(13):6532–6552, 2008.

[HP05] Darryl D. Holm and Vakhtang Putkaradze. "Aggregation of Finite-Size Particles with Variable Mobility." *Phys. Rev. Lett.*, **95**(22), Nov 2005. article 226106.

[HP06] Darryl D. Holm and Vakhtang Putkaradze. "Formation of clumps and patches in self-aggregation of finite-size particles." *Phys. D*, **220**(2):183–196, 2006.

[KPP37] A. N. Kolmogorov, I. G. Petrovskii, and N. S. Piskunov. "A study of the equation for diffusion combined with an increase of substance and its application to a problem in biology." *Bulletin Moskov. Univ. Mat. Mekh.*, **1**(6):1–26, 1937.

[KPV91] S. Kamin, L. A. Peletier, and J. L. Vázquez. "On the Barenblatt equation of elastoplastic filtration." *Indiana Univ. Math. J.*, **40**(4):1333–1362, 1991.

[KS70] E.F. Keller and L.A. Segel. "Initiation of slime mold aggregation viewed as an instability." *J. Theor. Biol.*, **26**:399415, 1970.

[KS10] Grzegorz Karch and Kanako Suzuki. "Blow-up versus global existence of solutions to aggregation equations.", 2010. arXiv:1004.4021.

[Lau07] Thomas Laurent. "Local and global existence for an aggregation equation." *Comm. Partial Differential Equations*, **32**(10-12):1941–1964, 2007.

[LR09] Dong Li and Jose Rodrigo. "Finite-time singularities of an aggregation equation in $\mathbb{R}^n$ with fractional dissipation." *Comm. Math. Phys.*, **287**(2):687–703, 2009.

[MB02] Andrew J. Majda and Andrea L. Bertozzi. *Vorticity and incompressible flow*, volume 27 of *Cambridge Texts in Applied Mathematics*. Cambridge University Press, Cambridge, 2002.

[MCO05] D. Morale, V. Capasso, and K. Oelschläger. "An interacting particle system modelling aggregation behavior: from individuals to populations." *Journal of mathematical biology*, **50**(1):49–66, 2005.

[ME99] Alexander Mogilner and Leah Edelstein-Keshet. "A non-local model for a swarm." *J. Math. Biol.*, **38**(6):534–570, 1999.

[MGF03] K. D. Moll, A. L. Gaeta, and G. Fibich. "Self-Similar optical wave collapse: Observation of the Townes profile." *Phys. Rev. Lett.*, **90**(20), May 2003. article 203902.

[MPS86] D. W. McLaughlin, G. C. Papanicolaou, C. Sulem, and P. L. Sulem. "Focusing singularity of the cubic Schrödinger equation." *Phys. Rev. A*, **34**(2):1200–1210, Aug 1986.

[MZ97] Frank Merle and Hatem Zaag. "Stability of the blow-up profile for equations of the type $u_t = \Delta u + |u|^{p-1}u$." *Duke Math. J.*, **86**(1):143–195, 1997.

[OL01] Akira Okubo and Simon A. Levin. *Diffusion and ecological problems: modern perspectives*, volume 14 of *Interdisciplinary Applied Mathematics*. Springer-Verlag, New York, second edition, 2001.

[PZ95] M. A. Peletier and Hong Fei Zhang. "Self-similar solutions of a fast diffusion equation that do not conserve mass." *Differential Integral Equations*, **8**(8):2045–2064, 1995.

[QS07] Pavol Quittner and Philippe Souplet. *Superlinear parabolic problems*. Birkhäuser Advanced Texts: Basler Lehrbücher. [Birkhäuser Advanced Texts: Basel Textbooks]. Birkhäuser Verlag, Basel, 2007. Blow-up, global existence and steady states.

[SGK95] A A. Samarskii, V A. Galaktionov, S P. Kurdyumov, and A P. Mikhailov. *Blow-up in quasilinear parabolic equations*, volume 19. Walter de Gruyter & Co., Berlin, 1995.

[SS99] C. Sulem and P.L. Sulem. *The nonlinear Schrödinger equation: self-focusing and wave collapse*. Springer Verlag, 1999.

[TB04] Chad M. Topaz and Andrea L. Bertozzi. "Swarming patterns in a two-dimensional kinematic model for biological groups." *SIAM J. Appl. Math.*, **65**(1):152–174 (electronic), 2004.

[Vaz07] Juan Luis Vázquez. *The porous medium equation: Mathematical theory*. Oxford Mathematical Monographs. The Clarendon Press Oxford University Press, Oxford, 2007.

[Vil03] Cédric Villani. *Topics in optimal transportation*, volume 58 of *Graduate Studies in Mathematics*. American Mathematical Society, Providence, RI, 2003.

[Yud63] V. I. Yudovich. "Non-stationary flow of an ideal incompressible liquid." *USSR Computational Mathematics and Mathematical Physics*, **3**(6):1407–1456, 1963.